Subunit organization and Rab interactions of Vps-C protein complexes that control endolysosomal membrane traffic

Rachael L. Plemel*, Braden T. Lobingier*, Christopher L. Brett, Cortney G. Angers, Daniel P. Nickerson, Andrew Paulsel, Debra Sprague, and Alexey J. Merz
Department of Biochemistry, University of Washington, Seattle, WA 98195-3750

ABSTRACT **Traffic through late endolysosomal compartments is regulated by sequential signaling of small G proteins of the Rab5 and Rab7 families. The *Saccharomyces cerevisiae* Vps-C protein complexes CORVET (class C core vacuole/endosome tethering complex) and HOPS (homotypic fusion and protein transport) interact with endolysosomal Rabs to coordinate their signaling activities. To better understand these large and intricate complexes, we performed interaction surveys to assemble domain-level interaction topologies for the eight Vps-C subunits. We identified numerous intersubunit interactions and up to six Rab-binding sites. Functional modules coordinate the major Rab interactions within CORVET and HOPS. The CORVET-specific subunits, Vps3 and Vps8, form a subcomplex and physically and genetically interact with the Rab5 orthologue Vps21. The HOPS-specific subunits, Vps39 and Vps41, also form a subcomplex. Both subunits bind the Rab7 orthologue Ypt7, but with distinct nucleotide specificities. The in vivo functions of four RING-like domains within Vps-C subunits were analyzed and shown to have distinct functions in endolysosomal transport. Finally, we show that the CORVET- and HOPS-specific subunits Vps3 and Vps39 bind the Vps-C core through a common region within the Vps11 C-terminal domain (CTD). Biochemical and genetic experiments demonstrate the importance of these regions, revealing the Vps11 CTD as a key integrator of Vps-C complex assembly, Rab signaling, and endosomal and lysosomal traffic.**

Monitoring Editor
Francis A. Barr
University of Liverpool

Received: Mar 29, 2010
Revised: Jan 7, 2011
Accepted: Feb 8, 2011

INTRODUCTION

Membrane traffic entails cycles of vesicle budding, transport, tethering, docking, and fusion with target membranes. These processes are regulated by the Rab-Arf family of small G proteins, which act as switches that confer specificity and directionality and as timers that control rates of membrane ingress and egress at each compartment. In current models, a patch of membrane moving (or maturing) through a sequence of compartments is signified by the presence of a specific associated Rab. As the patch matures, a handoff occurs in which one Rab is replaced by the next. This an arrangement is called a Rab cascade or relay (Grosshans *et al.*, 2006). Traffic through the endocytic-lysosomal pathway is controlled by members of the Rab5 and Rab7 families, which operate at earlier and later compartments, respectively. The Rab5-to-Rab7 handoff is controlled by signaling state of each Rab and by the Vps-C regulatory complexes CORVET and HOPS (Rink *et al.*, 2005; Peplowska *et al.*, 2007). The Rab5-to-Rab7 handoff is also controlled by a second evolutionarily unrelated complex, Mon1(SAND1)-Ccz1 (Kucharczyk *et al.*, 2001, 2009; Kinchen and Ravichandran, 2010; Nordmann *et al.*, 2010; Poteryaev *et al.*, 2010), which has also been called "HOPSII" (Wang *et al.*, 2003).

The Vps-C protein complexes were discovered in *S. cerevisiae* (Rieder and Emr, 1997; Srivastava *et al.*, 2000; Nickerson *et al.*, 2009). They contain a four-subunit core (Pep5/Vps11, Vps16, Pep3/Vps18, and Vps33) and two additional, compartment-specific subunits. CORVET, which contains the Vps-C core plus Vps3 and Vps8 (Raymond *et al.*, 1990; Horazdovsky *et al.*, 1996; Peterson and Emr, 2001; Peplowska *et al.*, 2007), operates at late endosomes and interacts with the Rab5 orthologue Vps21 (Horazdovsky *et al.*, 1996;

This article was published online ahead of print in MBoC in Press (http://www.molbiolcell.org/cgi/doi/10.1091/mbc.E10-03-0260) on February 16, 2011.

*These authors contributed equally to this work. All authors designed, performed, and analyzed experiments. A.J.M. and B.T.L. wrote the paper.

Address correspondence to: Alexey J. Merz (www.merzlab.org; merza@uw.edu).

Abbreviations used: ALP, alkaline phosphatase; CORVET, class C core vacuole/endosome tethering complex; CPS, carboxypeptidase S (Cps1); CPY, carboxypeptidase Y (Prc1); CTD, C-terminal domain; GEF, guanosine nucleotide exchange factor; GFP, green fluorescent protein; GST, glutathione S-transferase; HOPS, homotypic fusion and protein sorting complex; MVE, multivesicular endosome; RING, really interesting new gene; SNARE, soluble N-ethylmaleimide sensitive factor attachment protein receptor; TAP, tandem affinity purification; Y2H, yeast two-hybrid.

Peplowska *et al.*, 2007). HOPS, which contains the Vps-C core plus Vps39 (also called Vam6) and Vps41 (Seals *et al.*, 2000), operates at the lysosomal vacuole and interacts with the Rab7 orthologue Ypt7 (Seals *et al.*, 2000; Wurmser *et al.*, 2000; Brett *et al.*, 2008).

CORVET controls traffic into late endosomes, whereas HOPS controls all traffic—including late endosomes, autophagosomes, and Golgi-derived AP-3 vesicles—into the vacuole. Accordingly, the loss of any Vps-C core subunit results in the absence or malformation of all late-endosomal compartments, as well as severe conditional growth defects. Conversely, the loss of CORVET- or HOPS-specific subunits causes selective defects at late endosomes or vacuoles (Nickerson *et al.*, 2009). HOPS promotes Ypt7-dependent membrane tethering (Stroupe *et al.*, 2006) and SNARE-mediated membrane fusion (Sato *et al.*, 2000; Mima *et al.*, 2008). The HOPS subunit Vps39 was reported to be an activating guanosine nucleotide exchange factor (GEF) of Ypt7 (Binda *et al.*, 2009; Wurmser *et al.*, 2000), but more highly purified preparations of Vps39 and HOPS do not exhibit intrinsic nucleotide exchange activity toward Ypt7 (Nordmann *et al.*, 2010; Ostrowicz *et al.*, 2010; Lobingier, Brett, and Merz, unpublished data). Moreover, strong genetic (Kucharczyk *et al.*, 2000, 2001; Wang *et al.*, 2002) and biochemical (Nordmann *et al.*, 2010) evidence indicates that another complex, Mon1-Ccz1, is a bona fide Ypt7 GEF. The Vps41 subunit of HOPS directly interacts with Ypt7, and it is essential for stable HOPS binding to Ypt7-GTP (Brett *et al.*, 2008). Functions analogous to HOPS have been proposed for CORVET (Peplowska *et al.*, 2007), although CORVET is not known to tether membranes directly or to promote SNARE assembly. Hybrid complexes containing both CORVET- and HOPS-specific subunits (Peplowska *et al.*, 2007) raise the possibility that Vps-C complexes are remodeled on-the-fly, concomitantly with the endolysosomal Rab cascade. However, dynamic subunit exchange has been neither demonstrated nor linked to specific endolysosomal trafficking events.

Here we present domain-level dissections of Vps-C subunit interactions with one another and with Rab small G proteins. We employ yeast two-hybrid (Y2H) miniarrays to systematically search for Vps-C subunit–subunit and subunit–Rab contacts and purify three dimeric subassemblies. Two subassemblies are composed of HOPS- or CORVET-specific subunits; we show that they function as integrated Rab-interaction modules. Through genetic analyses, we show that the core subunit Vps11 is a key scaffold for Vps-C complex assembly and demonstrate that its C-terminal domain (CTD) is of special importance, physically and functionally linking the HOPS and CORVET Rab-interaction modules to the Vps-C core.

RESULTS

Domain architecture of Vps-C subunits

We analyzed yeast and human Vps-C subunits using the ROBETTA suite of structure prediction algorithms (Kim *et al.*, 2004; Chivian *et al.*, 2005). Previously, ~200 residues of sequence homology to clathrin proximal leg were detected in C-terminal regions of Vps8, Vps11, Vps18, Vps39, and Vps41 (Conibear and Stevens, 1998; Ybe *et al.*, 1999). Vps39 was reported to contain a short motif similar to a COPI (coat protein complex I) outer-shell coat subunit (Conibear and Stevens, 1998). Vps41 was shown to contain WD40 motifs (repeats of ~40 residues, often terminating in W and D), which typically form β-propellers (Rehling *et al.*, 1999). Our analyses (Figure 1 and Supplemental Table 1; Nickerson *et al.*, 2009) revealed a pervasive similarity to vesicle coat and nuclear pore proteins: seven of eight subunits contain a predicted N-terminal β-propeller followed by a C-terminal α-solenoid. In addition, Vps8, Vps11, and Vps18 have C-terminal RING (really interesting new gene) motifs, and Vps39 has a partial RING motif, although this region lacks residues that would

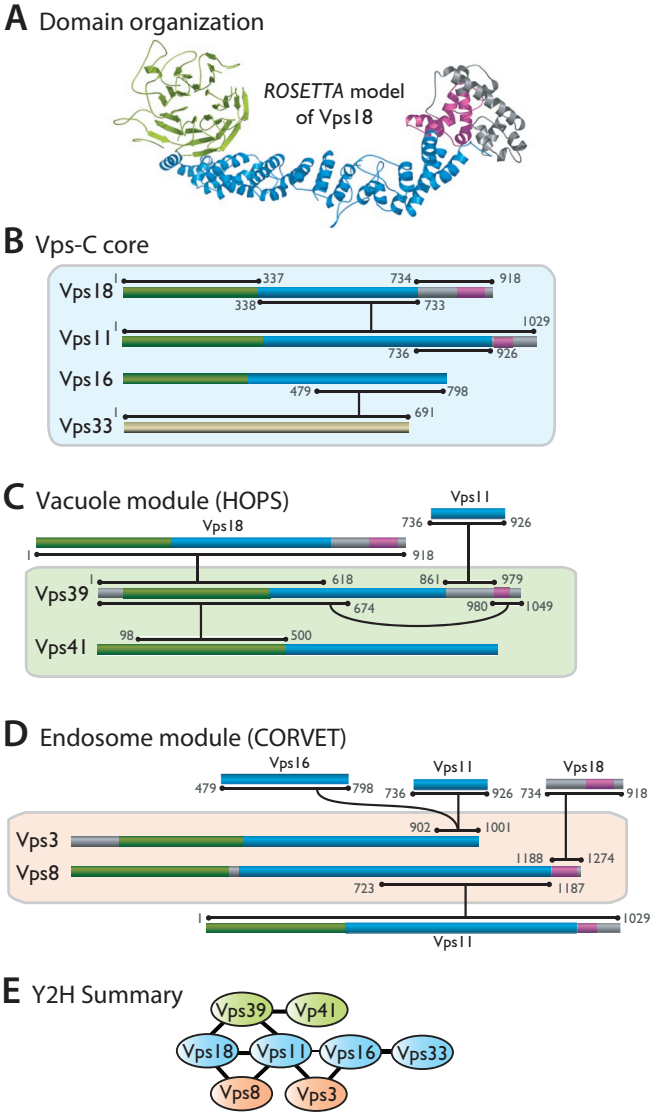

FIGURE 1: Vps-C domain structure and intersubunit interactions detected in Y2H screens. Structure predictions are color-coded consistent with the predicted structure of Vps18. (A) Predicted β-propellers are shaded green. Predicted α-solenoids are shaded blue. RING or RING-like motifs are shaded magenta. (B–D) Summary of Y2H interactions. Horizontal bars at each end of an interaction line delineate the minimal region of each protein sufficient to support a Y2H interaction, with numbers denoting the termini of these regions. In many cases larger segments also supported each interaction (Supplemental Table S2). (E) Summary of the overall interaction topology. The thinner line between Vps11 and Vps16 denotes a weak interaction not observed in all experiments.

coordinate a second Zn^{2+} ion. Similar predictions were obtained for human and yeast orthologues (Supplemental Table 1). These findings provided the basis for our domain-level dissection of Vps-C subunits.

Domain-level interaction topology of Vps-C complexes

HOPS and CORVET are sufficiently stable to withstand affinity isolation, chromatographic purification, and sedimentation (Rieder and Emr, 1997; Seals *et al.*, 2000; Stroupe *et al.*, 2006; Peplowska *et al.*, 2007; Angers and Merz, 2009), but only a few direct intersubunit contacts have been identified, using disparate approaches and

organisms. To obtain a broader inventory of intersubunit contacts, we performed exhaustive Y2H analyses.

Y2H can be very sensitive, potentially reporting bridging interactions mediated by proteins not encoded by the query constructs, so we used a de-tuned Y2H system originally designed to minimize false-positive signals in high-throughput screens (Uetz *et al.*, 2000). This system uses single-copy bait and prey vectors rather than the more commonly used multicopy vectors. Recent quantitative assessments demonstrate that use of single-copy Y2H vectors, in combination with the *HIS3* reporter gene and 3-aminotriazole (3-AT) in colony growth assays, nearly eliminates false-positive signals in Y2H interaction experiments (Venkatesan *et al.*, 2009; Chen *et al.*, 2010). Identical highly stringent assay conditions were used throughout the present study.

The Y2H-derived Vps-C interaction topology is summarized in Figure 1; the full results are reported in Supplemental Table S2. Our survey replicated (and in most cases mapped to higher resolution) almost all published interactions within Vps-C complexes across all organisms studied to date (Nakamura *et al.*, 1997; Sevrioukov *et al.*, 1999; Srivastava *et al.*, 2000; Wurmser *et al.*, 2000; Peterson and Emr, 2001; Pulipparacharuvil *et al.*, 2005; Peplowska *et al.*, 2007). This finding suggests that not only the subunit folds but also the interaction topologies and functional dynamics of Vps-C complexes are broadly conserved. Our survey also revealed candidate interactions that to our knowledge have not previously been reported. The minimal regions sufficient for each interaction are largely nonoverlapping, strongly suggesting that most interactions detected in this survey are direct rather than bridged through other subunits.

Vps11, particularly in its C-terminal region, is a densely connected hub (Figure 1E), interacting with Vps18, Vps8, Vps3, and Vps39. Vps39 and Vps3 share substantial sequence homology, with the region of highest similarity within a stretch of ~100 residues near their C-termini. The Vps3 and Vps39 CTDs interacted strongly with residues 736–926 in the Vps11 CTD, suggesting that they may bind to a single site within Vps11 (Figure 1, C and D). The HOPS subunit Vps39 also interacts with the HOPS subunit Vps41. The Vps39–Vps41 interaction was relatively weak, but it was detected in both bait–prey and prey–bait configurations; this was the strongest interaction detected between Vps41 and any other HOPS subunit.

Isolation of three Vps-C subcomplexes

To examine the ability of subunits to heterodimerize in the absence of the HOPS and CORVET holocomplexes, pairs of subunits were coexpressed in insect cells. In each case, one subunit was expressed as a glutathione S-transferase (GST) fusion, the other as a His_6 fusion, and complexes were purified using the two affinity tags in sequence. From several tested pairs, three subcomplexes were identified (Figure 2). Vps16 is required for Vps33 association with Vps11 and Vps18 (Rieder and Emr, 1997), and a region corresponding to yeast Vps16 residues 451–595 mediates binding between *Drosophila* Vps16A and B and Vps33A and B (Pulipparacharuvil *et al.*, 2005). Our Y2H survey mapped an overlapping site within Vps16 (residues 479–798; Figure 1) and indeed Vps16 and Vps33 form a subcomplex when coexpressed (Figure 2A). The CORVET subunits Vps3 and Vps8 also form a subcomplex (Figure 2B). This binding interaction has not to our knowledge been reported previously, and it was not detected in our Y2H survey. Like Vps3 and Vps8, the HOPS subunits Vps39 and Vps41 formed a binary complex (Figure 2, C and D); the interacting domains were mapped by Y2H to the N-termini of both proteins (Figure 1C; Supplemental Table S2). The Vps39 CTD was sufficient to interact with Vps11 and was necessary for stable Vps39 association with HOPS (Figure 1; Supplemental Table S2; Wurmser *et al.*, 2000). However, the Vps39 CTD was not needed for Vps39 binding to Vps41 (Figure 2D). Both subcomplexes exhibited signs of lability, suggesting that their interactions are stabilized when they reside within the HOPS and CORVET holocomplexes.

Y2H identification of Vps-C Rab-interaction sites

CORVET interacts with the Rab5 orthologue Vps21, and HOPS interacts with the Rab7 orthologue Ypt7. Vps39 binds GDP- or GTP-Ypt7 and was previously reported to harbor Ypt7 GEF activity (Wurmser *et al.*, 2000; Binda *et al.*, 2009). Vps41 binds directly to Ypt7 and is essential for stable binding of HOPS to Ypt7-GTP (Brett *et al.*, 2008). Until recently, no Rab-binding sites were definitively identified within CORVET, although there was genetic evidence that Vps3 and Vps8 contribute to the CORVET Vps21 binding activity (Horazdovsky *et al.*, 1996; Peplowska *et al.*, 2007; Markgraf *et al.*, 2009; Pawelec *et al.*, 2010). To identify Rab-binding sites, Y2H miniarrays comprising the 11 yeast Rabs were prepared. In addition to wild-type Rabs, Rab point mutants were included in the arrays, including mutants favoring specific nucleotide states or lacking C-terminal sites of covalent prenylation (lipid-free). Rab miniarrays were used to probe Vps-C miniarrays in both bait and prey configurations (Supplemental Table S3). At least six candidate interactions were identified by Y2H. Vps21 interacted with CORVET subunits Vps3 and Vps8, and with the N-terminal domain of Vps-C core subunit Vps11 (Supplemental Table S3). Ypt7 interacted with HOPS subunits Vps39 and Vps41 (Figure 3A; Supplemental Table S3; Brett *et al.*, 2008; Wurmser *et al.*, 2000) and weakly with the core subunit Vps33.

The HOPS–Ypt7 interaction module

In pulldowns, native HOPS interacts preferentially with Ypt7-GTPγS versus Ypt7-GDP (Price *et al.*, 2000; Seals *et al.*, 2000; Peplowska *et al.*, 2007; Brett *et al.*, 2008). However, under conditions that yielded highly selective binding of native HOPS to Ypt7-GTP, there was no GTP versus GDP selectivity when purified Vps41 was tested. Further studies indicated that nucleotide stripping under our previous conditions was inefficient. With a more stringent strip-exchange procedure, purified Vps41 selectively bound Ypt7-GTPγS (Figure 3B and Supplemental Figure S1), establishing Vps41 as a direct effector of Ypt7-GTP and explaining why it is required (Brett *et al.*, 2008) for the stable association of HOPS with Ypt7-GTP.

In previous studies, Vps39 was reported either to bind Ypt7-GDP (Wurmser *et al.*, 2000) or to show no nucleotide selectivity (Brett *et al.*, 2008). Under our improved nucleotide-loading conditions, purified Vps39–860Δ bound Ypt7 without any detectable GNP selectivity (Figure 3, C and D). Taken together, our Y2H and biochemical data show that the N-terminal predicted β-propellors of Vps39 and Vps41 interact with one another and with the vacuolar Rab Ypt7, with Vps41 showing strong selectivity for Ypt7-GTP and Vps39 showing little or no nucleotide selectivity. Because Vps39 was the only HOPS subunit that interacted with Vps41 in our Y2H experiments, we asked whether Vps41 could remain associated with the remaining HOPS subunits in the absence of Vps39. Coimmunoprecipitation experiments using anti-Vps11 antibodies (Figure 3E) demonstrated that the five remaining HOPS subunits remain stably associated in the absence of Vps39. This result indicates that, in addition to Vps39, Vps41 has additional binding interactions with the core that were not detected in our Y2H survey. In contrast to Vps39, the core subunit Vps18 has a crucial role in the assembly of HOPS and the Vps-C core, because deletion of Vps18 prevented

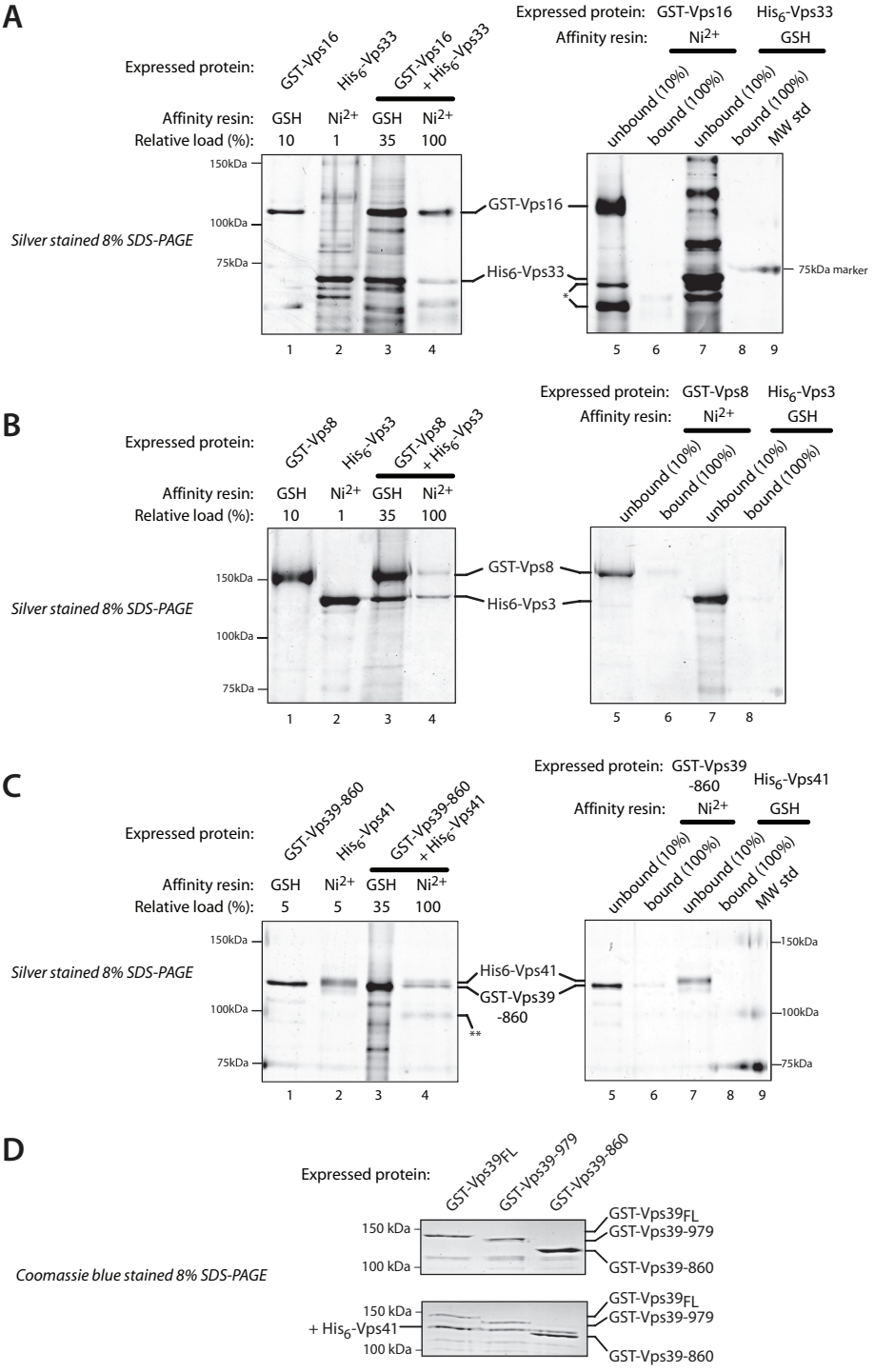

FIGURE 2: Purification of Vps-C subcomplexes. (A–C) The indicated subunits were expressed individually or in pairs in insect cells and isolated by affinity chromatography. In each panel, the gel on the left shows isolation of a subcomplex, while the gel on the right shows pulldown specificity controls. Lanes 1 and 2, GST-tagged or His_6-tagged subunits were expressed individually and purified on either Ni^{2+}-NTA resin (Ni^{2+}) or glutathione-agarose (GSH) resin. Lanes 3 and 4, pairs of GST- and His_6-tagged subunits were coexpressed, captured on GSH resin and eluted with reduced glutathione (lanes 3), and then recaptured on Ni^{2+} resin (lanes 4). Lanes 5–8, pulldown specificity controls showing that Ni^{2+}-NTA beads retain little or no GST fusion protein, and that glutathione-sepharose beads (GSH) retain little or no His_6 fusion protein when these proteins are expressed individually (i.e., in the absence of an interacting partner whose tag can bind the affinity resin). Lanes 6 and 8, material retained on the noncognate affinity beads. Lanes 5 and 7, unbound (flowthrough) material. The SDS–PAGE gels were sliver-stained. (D) Copurification of His_6-tagged Vps41 associated with GST-Vps39 or GST-Vps39 truncation mutants.

coimmunoprecipitation of Vps11 and Vps16, Vps18, Vps33, or Vps41 (Figure 3E).

As the region of Vps39 required for its interaction with Vps11 maps to the Vps39 C-terminus (residues 860–979) (Supplemental Table S2; Wurmser *et al.*, 2000), we analyzed the in vivo phenotypes of two C-terminal Vps39 deletion mutants. In vivo homotypic fusion was evaluated by examining vacuole morphology with the endocytic tracer dye FM4-64 (Figure 4A). Traffic to the vacuole was evaluated by subcellular fractionation followed by immunoblotting for two cargo proteins, CPY (carboxypeptidase Y, Prc1) and alkaline phosphatase (ALP) (Figure 4B). In this procedure, Golgi membranes and small vesicles fractionate to the 100,000 × *g* pellet (P100). Endosomes are found in the 13,000 × *g* pellet (P13) and P100 fractions. Vacuoles are found in the P13 fraction almost exclusively. Immunoblotting of fractions with fiduciary markers for vacuolar, endosomal, and soluble markers was performed for each experiment, and proper fractionation was confirmed for each mutant (unpublished results). CPY is transported from the late Golgi to endosomes, and then to the vacuole. ALP is delivered from the Golgi to the vacuole through the AP-3 pathway, which bypasses endosomes. Both ALP and CPY are synthesized as inactive proenzymes (p) that are proteolytically processed into active mature (m) enzymes upon arrival at the vacuole. Transport defects result in the accumulation of slow-migrating ALP or CPY proenzymes in the P100 and P13 fractions (Figure 4B).

The *vps39–860*Δ mutation completely phenocopies the defects in CPY and ALP localization and maturation, and vacuole morphology, conferred by *vps39*Δ or *vps41*Δ mutations (Figure 4; Supplemental Table S2; Brett *et al.*, 2008). In contrast, *vps39–979*Δ mutant cells produce Vps39 with an intact Vps11-binding site and exhibit only mild trafficking defects (Figure 4; Supplemental Table S4). Expression of Vps39–860 from an ectopic promoter results in higher levels of Vps39–860Δ than Vps39 wild type (unpublished results), indicating that the loss of function in the *vps39–860*Δ mutant is not due to poor expression or accelerated turnover of Vps39–860Δ protein. Because Vps39 residues 860–979 are necessary and sufficient for Vps39 binding to Vps11 and Vps39 association with HOPS, but not required for Vps39 interactions with Ypt7 or Vps41, our results suggest that Vps39 function depends on its interactions with HOPS through both Vps11 and Vps41. We conclude that the Vps39–Vps41 subcomplex is a physically and functionally integrated effector module

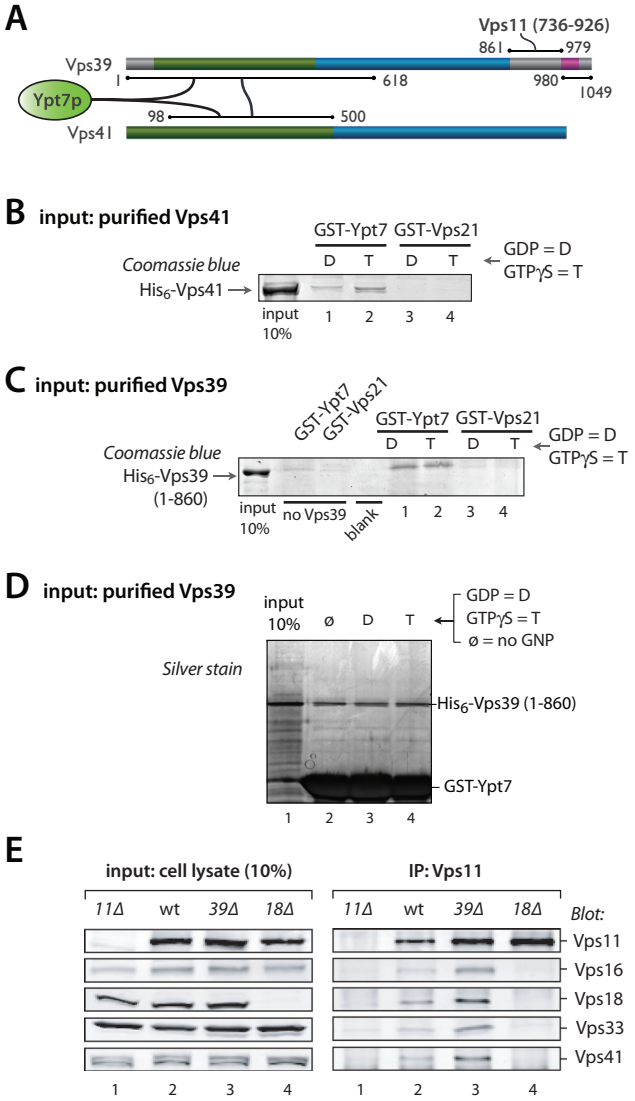

FIGURE 3: HOPS subunits Vps39 and Vps41 form an integrated Ypt7 activation and binding module. (A) Summary of key Vps39 and Vps41 interactions (see Supplemental Tables S2 and S3 for full results). (B) Direct binding of Vps41 to Ypt7. Pulldowns were performed using purified recombinant His_6-Vps41 and beads decorated with either GST-Ypt7 or GST-Vps21. The Rabs were nucleotide-loaded by procedure 2 (see *Materials and Methods* and Supplemental Figure S1). (C) Direct binding of Vps39 to Ypt7. Pulldowns were performed using purified recombinant His_6-Vps39–860Δ and beads decorated with either GST-Ypt7 or GST-Vps21. The Rabs were nucleotide-loaded by procedure 2 (see *Materials and Methods*). (D) Vps39 binds Ypt7 without nucleotide selectivity. GST-Ypt7 was nucleotide-stripped by procedure 2 (see *Materials and Methods*), then loaded with GDP, GTPγS, or no nucleotide. Beads decorated with the resulting GST-Ypt7 were then used to pull down His_6-Vps39 (1–860). No differences in binding efficiency were observed.

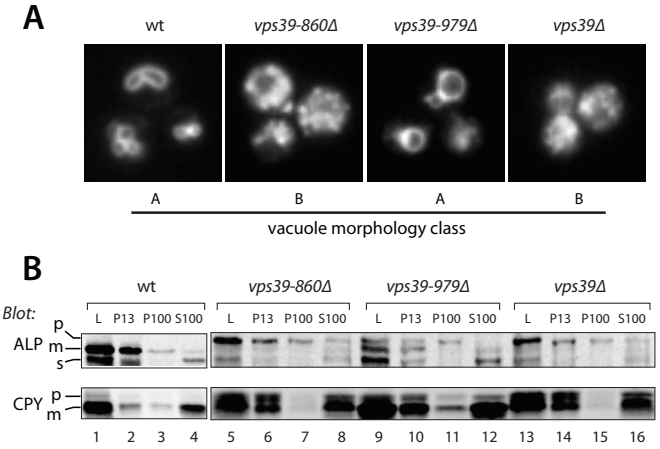

FIGURE 4: In vivo phenotypes of Vps39 C-terminal truncation mutants. (A) Vacuole morphology phenotypes of *vps39* mutant cells. Vacuoles were labeled by pulse-chase with the tracer dye FM4–64 and examined by fluorescence microscopy. (B) Differential centrifugation analyses of ALP and CPY maturation and subcellular localization in *vps39* mutant cells. L, cell lysate; P13 and P100, 13,000 × *g* and 100,000 × *g* pellets; S100, 100,000 × *g* supernatant. Vacuoles are found almost entirely in the P13 fraction. Small vesicles and Golgi membranes are found in the P100 fraction. Soluble proteins and complexes (including CPY and the soluble ALP cleavage product, sALP, released from the lumens of vacuoles that ruptured during fractionation) are found in the S100 fraction. For each strain, 50 OD_{600} ml were lysed and subjected to differential centrifugation (see *Materials and Methods*), and the fractions were analyzed by immunoblotting with monoclonal antibodies against ALP (Pho8) or CPY (Prc1). The cell lysate load fraction (L) corresponds to 20% of the other fractions. p = proenzyme, m = mature enzyme, s = soluble. The results of these assays, and of CPY-invertase secretion assays, are summarized in Supplemental Table S2.

containing two Ypt7-binding sites with distinct nucleotide specificity. These sites reside within N-terminal predicted β-propellors that physically interact with one another.

The CORVET–Vps21 interaction module

In Y2H assays the two CORVET subunits, Vps3 and Vps8, interacted with wild-type Vps21 and Vps21-Q66L (GTP hydrolysis-deficient), but not with Vps21-S21L (a GDP-biased mutant) or any other *Saccharomyces* Rab (Figure 5, A and B; Supplemental Table S3). Additional controls validated the Y2H Rab constructs: the Vps21 effector Vac1 (Peterson *et al.*, 1999) had Rab interaction patterns identical to Vps3 and Vps8, whereas the Vps21 GEF Vps9 interacted strongly with Vps21-S21L but not with wild-type Vps21 or Vps21-Q66L (Hama *et al.*, 1999; Plemel and Merz, unpublished data). Vps3, like Vps41 and Vps39, interacted with its cognate Rab thorough a predicted N-terminal β-propeller. In contrast, Vps8 interacted with Vps21 through the Vps8 C-terminal predicted α-solenoid (Figure 5A; see also Pawelec *et al.*, 2010). The Vps3–Vps21 interaction was validated biochemically. Vps3 in cell lysates, presumably as a subunit of CORVET, bound to Vps21-GTPγS with high specificity (Figure 5C; Peplowska *et al.*, 2007). Moreover, purified Vps3 bound to Vps21 with strong selectivity for Vps21-GTPγS versus -GDP (Figure 5D). These experiments suggest that both Vps3 and Vps8 contain Vps21-binding sites, and establish that Vps3 is a direct, GTP-selective effector of Vps21.

The Vps3 CTD is highly homologous to the Vps39 CTD. As with Vps39, the Vps3 CTD is required for its interaction with the Vps11 CTD, and as with the Vps39 CTD it is functionally indispensable: deletion of the Vps3 CTD (*vps3–901Δ*) phenocopied the vacuole morphology and trafficking defects of a *vps3Δ* null mutant (Figure 5E and Supplemental Table S4). Thus homologous CTDs within Vps3 and Vps39 are essential for the functions of both proteins and bind an ~190-residue region within the Vps11 CTD.

Genetic suppression experiments show that the Vps8–Vps21 interaction detected by Y2H (Figure 5, A and B; Supplemental Table

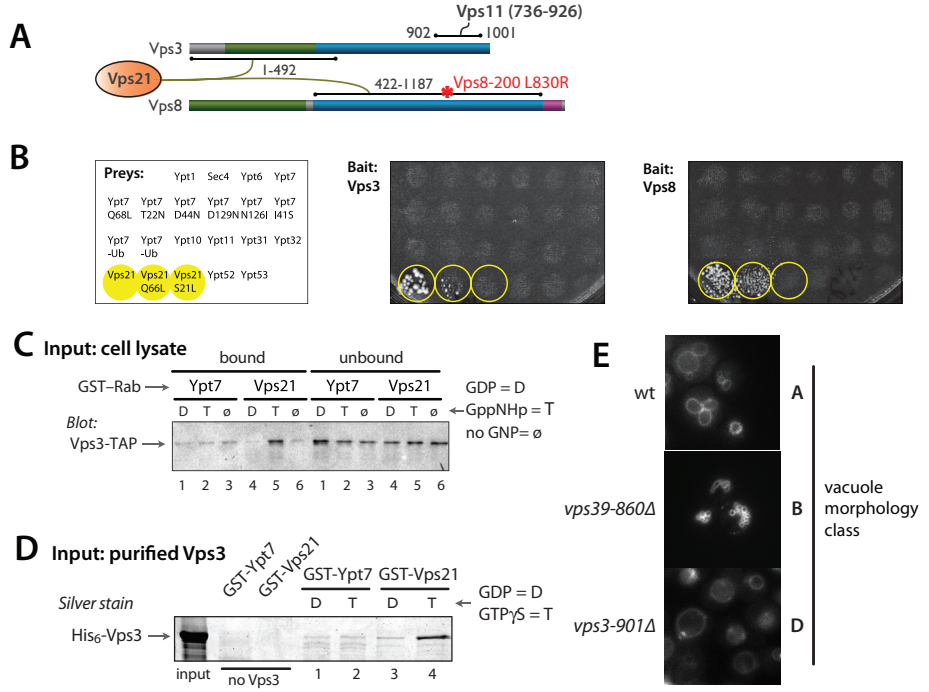

FIGURE 5: CORVET subunits Vps3 and Vps8 are a Vps21 interaction module. (A) Summary of Vps3 and Vps8 Y2H interactions. The position of the L830R mutation in the *VPS8–200* mutant is indicated. (B) Vps3 and Vps8 interact with Vps21-GTP in Y2H miniarray experiments. The prey strains are indicated at left and were mated with strains containing either (middle) Vps3 or (right) Vps8 bait constructs. Yeast colony growth on synthetic medium (-Trp, -Leu, -His, +3-AT) indicates a positive Y2H interaction. Note that Vps3 and Vps8 interacted with Vps21 and the GTP-biased mutant Vps21-Q66L but did not interact with any Rab other than Vps21 and did not interact with the GDP-biased Vps21-S21L mutant. (C) Native Vps3 in yeast cell lysates is selectively retained on a Vps21-GTP affinity resin. Note that most Vps3 in cell lysates is found within the CORVET complex. A similar pulldown, employing purified Vps3 rather than a cell lysate, is shown in Figure 4B. Cell lysates were prepared as described previously (Brett *et al.*, 2008). TAP (tandem affinity purification)-tagged Vps3 was identified by immunoblotting with peroxidase-antiperoxidase (Upstate-Millipore, Billerica, MA). (D) Vps3 binds directly to Vps21-GTP. GST pulldown experiments were performed using purified recombinant His_6-Vps3 and beads decorated with GST-Ypt7 or GST-Vps21 loaded with GDP or GTPγS by procedure 2 (*Materials and Methods*). (E) In vivo vacuole morphology of strains carrying Vps3 and Vps39 truncations that cannot interact with the Vps11 CTD. Vacuoles were stained using an FM4–64 pulse-chase (*Materials and Methods*).

S3) is functionally important and suggest that the Vps8–Vps21 interaction is, like the Vps3–Vps21 interaction, direct. Truncation of Vps11 to residue 445 causes conditional growth defects, complete defects in biosynthetic traffic to late endosomes and vacuoles (Figure 6A; Woolford *et al.*, 1998), and class C vacuole morphology (Figure 6B). The *VPS88–200* allele suppresses several of these *vps11–445*Δ phenotypes: it rescues growth defects, restores endosomal (but not vacuolar) trafficking, and results in a class B vacuole morphology similar to *vps39*Δ, *vps41*Δ, or *ypt7*Δ mutant cells (Figure 6, A and B; Woolford *et al.*, 1998). In Y2H screens we found that Vps21 interacted more strongly with Vps8–200 than with wild-type Vps8 (Figure 6C). This difference in interaction strength was not attributable to differences in the expression of the Vps8 and Vps8–200 prey constructs (Figure 6D). The same enhanced interaction was observed in reciprocal experiments where Vps21 was used as the prey and Vps8 or Vps8–200 were used as baits (Supplemental Figure S2A). Moreover, neither GTP preference nor selectivity for Vps21 versus other Rabs was modified by the Vps8–200 mutation, and the difference between Vps8 and Vps8–200 was seen with either full-length constructs or with truncated constructs containing the Vps21-binding region (Figure 6C and Supplemental Figure S2B). We sequenced *VPS8–200* and identified a single missense substitution at an evolutionarily conserved residue (L830 to R), which is near the middle of the Vps21 interaction region (Figure 5A). Taken together, our results indicate that Vps21 interacts with both Vps3 and Vps8, and suggest a biochemical basis—enhanced Vps21 binding to Vps8—for the genetic suppression of *vps11–445*Δ trafficking phenotypes by *VPS8–200*.

The Vps11 CTD organizes Vps-C assembly and signaling

Among the Vps-C subunits, Vps11 had the densest web of interactions with other subunits, particularly within its CTD (Figure 7A). Notably, both the CORVET-specific subunit Vps3 and its HOPS-specific paralogue Vps39 interact via their conserved CTDs with the Vps11 CTD; these regions in Vps3 and Vps39 are functionally indispensable (Figures 4 and 5E; Supplemental Table S4). To dissect the functional architecture of the Vps11 CTD, we prepared a set of Vps11 truncation alleles (Figure 7A) and evaluated their in vivo phenotypes.

Each *vps11* allele was prepared as a chromosomal replacement driven by the *VPS11* promoter. *vps11*Δ null mutants exhibited defects in endosomal delivery indicated by pro-CPY accumulation and CPY secretion into the extracellular medium (Figure 7B and Supplemental Table S4), defects in vacuolar delivery indicated by accumulation of pro-ALP and pro-CPY, and defects in late endosome and vacuole fusion, indicated by class C vacuole morphology (Figure 7C). Four C-terminal Vps11 truncations (350Δ, 445Δ, 505Δ, and 735Δ) completely phenocopied the *vps11*Δ null allele (Figure 7, B and C; Supplemental Table S4). The total loss of function in the *VPS11–735*Δ mutant is particularly important, because this mutant lacks binding sites for Vps3 and Vps39 (Figure 7A).

In contrast to the more severe truncation mutants, a mutant lacking the Vps11 RING motif (*vps11–926*Δ) exhibited relatively selective defects: slightly impaired CPY processing and limited CPY secretion from the cell, but a severe defect in ALP processing (Figure 7B and Supplemental Table S4). These phenotypes are diagnostic of defective docking or fusion at the vacuole, but not at the endosome. Consistent with this interpretation, *vps11–926*Δ cells had class B fragmented vacuoles similar to *vps39*Δ or *vps41*Δ cells (Figure 7C). Because the Vps11 RING motif interacted weakly with other Vps-C subunits including Vps16 (Supplemental Table S2), coimmunoprecipitation experiments were performed to ascertain whether HOPS is intact in *vps11–926*Δ mutant cells (Figure 5D). The results show that Vps11, Vps16, Vps18, and Vps41 all coprecipitate at least as efficiently with Vps11–926Δ as with wild-type Vps11. Together, these results indicate that the Vps11 RING is not needed for HOPS complex assembly but instead functions predominantly to regulate fusion at the vacuole, presumably through binding interactions with other HOPS subunits or interactions with other fusion factors.

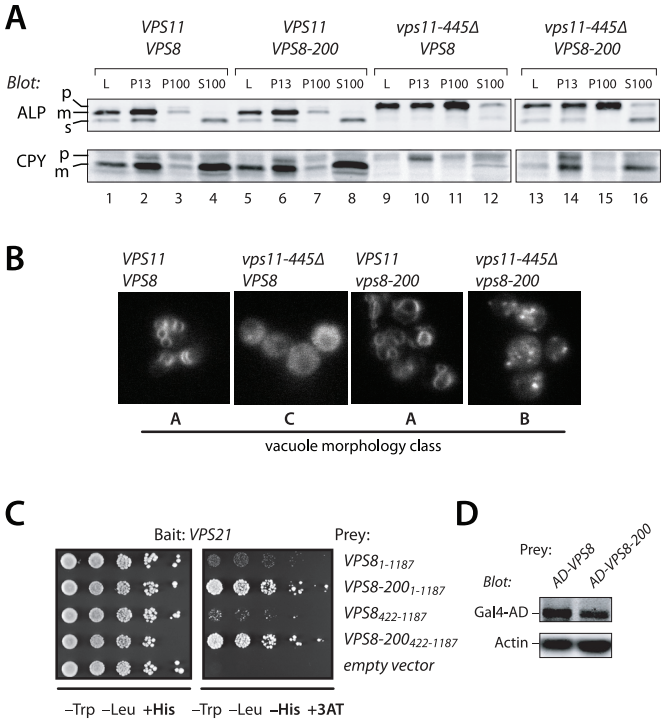

FIGURE 6: Genetic suppression reveals functional interactions between Vps8 and Vps21. (A) Differential centrifugation analysis of ALP and CPY maturation and subcellular localization in cells carrying *vps11–445Δ* and *VPS8–200* alleles. (B) Vacuole morphology phenotypes of *vps11–445Δ and VPS8–200* mutant cells. Vacuoles were visualized by pulse-chase with the fluorescent dye FM4–64 and examined by fluorescence microscopy. Assays were performed as in Figure 4B. (C) Vps8–200 is a hyperactive Vps21 interactor in Y2H assays. More robust growth on media lacking His and supplemented with 3-aminotriazole (3-AT) indicates a stronger Y2H interaction. Limiting dilution analysis is shown for each Y2H reporter strain, with serial fivefold dilutions plated from left to right. (D) Differences in protein expression do not explain enhanced Y2H interactions between Vps8–200 and Vps21. Immunoblot analysis of the AD-Vps8 and AD-Vps8–200 Y2H prey constructs used in Figure 1D show that AD-Vps8–200 is expressed at identical or lower levels compared with AD-Vps8. The immunoblots were also probed with anti-actin as a gel loading control.

In addition to Vps11, three other Vps-C subunits contain RING/Zn^{2+} finger motifs at their extreme C-termini (see Figure 1 and Supplemental Table 1). We compared the functions of these motifs by deleting each one; all are functionally important. The severity of the trafficking defects observed in each ΔRING/Zn^{2+} finger mutant, from most severe to least, was as follows: *vps18–826Δ* > *vps11–926Δ* > *vps39–979Δ* *vps8–1188Δ* (Supplemental Table S2; Figures 4B and 7B). The Vps8 and Vps18 RING domains appear to heterodimerize (Figure 1; Supplemental Table S2). However, the more severe vacuolar and endosomal defects observed upon deletion of the Vps18 RING versus the Vps8 RING indicate that Vps8 cannot be the sole functional target of the Vps18 RING. Vps39 might be capable of a self-interaction mediated through its RING-like domain (Figure 1C). Weak Y2H interactions were sometimes detected between the Vps11 RING and other subunits, including Vps16 (Supplemental Table S2). Taken together, these data show that the four Vps-C RING/Zn^{2+} finger motifs have distinct functions in endolysosomal trafficking.

The Vps11 CTD (residues 736–926) interacts with ~100-residue CTDs of high similarity in Vps3 and Vps39, so we asked whether the *vps11–735Δ* truncation might be complemented in trans by the missing Vps11-(736–1029) fragment. Remarkably, coexpression of this fragment rescued the vacuole morphology (Figure 8A) of both *vps11–736Δ* and *vps11–936Δ* cells, but it failed to rescue in *vps11–350Δ*, *-445Δ*, or *-505Δ* cells. Identical rescue results were obtained with expression of green fluorescent protein (GFP)-tagged or untagged Vps11-(736–1029). The CPY and ALP maturation defects of *vps11–735Δ* cells were also rescued by Vps11-(736–1029) (Figure 8B; Supplemental Table S4). We also evaluated the formation of multivesicular endosomes (MVEs) in *vps11–735Δ* cells expressing Vps11-(736–1029). GFP-CPS (carboxypeptidase S, Cps1) is sorted through the MVE pathway into the vacuole lumen. Defects in the formation of MVEs result in missorting of GFP-CPS to the vacuole limiting membrane. The two-fragment complemented strain correctly sorted GFP-CPS to the vacuole lumen, indicating that MVE function is intact in these cells (Supplemental Table S4). Together, the results indicate that endolysosomal traffic is essentially normal in cells expressing both Vps11-(735Δ) and Vps11-(736–1029).

In every *vps11* mutant strain tested, the GFP-Vps11-(736–1029) fragment exhibited a discrete subcellular localization (Figure 8A). In *vps11–735Δ* or *vps11–926Δ* cells, it localized predominantly to the vacuole limiting membrane and to perivacuolar foci, which are probably late endosomes. In *vps11–350Δ*, *-445Δ*, and *-505Δ* cells, GFP-Vps11-(736–1029) usually localized to a single bright punctate spot. In wild-type cells, however, GFP-Vps11-(736–1029) was exclusively cytoplasmic, indicating that the C-terminus of native Vps11 saturates the site(s) required for localization of Vps11-(736–1029). This was confirmed in coimmunoprecipitation experiments (Figure 8C). GFP-Vps11-(736–1029) coprecipitated Vps16, Vps18, Vps33, and Vps41 in the truncation mutants (Figure 8C, lanes 2–6). In cells containing full-length Vps11, coisolation of other subunits with GFP-Vps11-(736–1029) was almost eleminated (Figure 8C, lanes 1), consistent with its diffuse localization in *VPS11* cells (Figure 8A). Together, these data show that Vps11 can be split in two and retain nearly its full function. However, in the absence of a central domain (e.g., when 1–505 and 736–1029 are coexpressed), the phenotype is equivalent to a *vps11Δ* null, even though a HOPS complex of apparently normal composition is assembled (Figure 8C, lanes 4 and 5). Thus the central domain (residues 351–735) is also crucial for Vps11 function. The split N- and C-terminal fragments of Vps11 probably assemble on Vps18 (Figure 7A). This conclusion is supported by our finding that the integrity of the entire wild-type complex is lost when Vps18 is deleted (see Figure 3E, lanes 4). Taken together, these experiments underscore the complex and critical functions of the Vps11 CTD in both HOPS and CORVET function.

DISCUSSION

Our main conclusions are that the CORVET subunits Vps3 and Vps8, and the HOPS subunits Vps39 and Vps41, form discrete complex-specific subassemblies that function in Rab recognition. The activities of these subassemblies are coordinated with the core through contacts between the CTDs of Vps3 or Vps39 and the CTD of Vps11. The core subunits Vps16 and Vps33 also form a stable subassembly. Vps33 belongs to the Sec1-Munc18 (SM) family of cofactors (Sudhof and Rothman, 2009), which are universally required for SNARE-mediated membrane fusion, so Vps16 and Vps33 likely link the Rab signaling activities of HOPS and CORVET to SNARE-mediated membrane fusion.

In early studies, HOPS was identified as an effector of Ypt7-GTP (Price *et al.*, 2000; Seals *et al.*, 2000) and the Vps39 subunit was

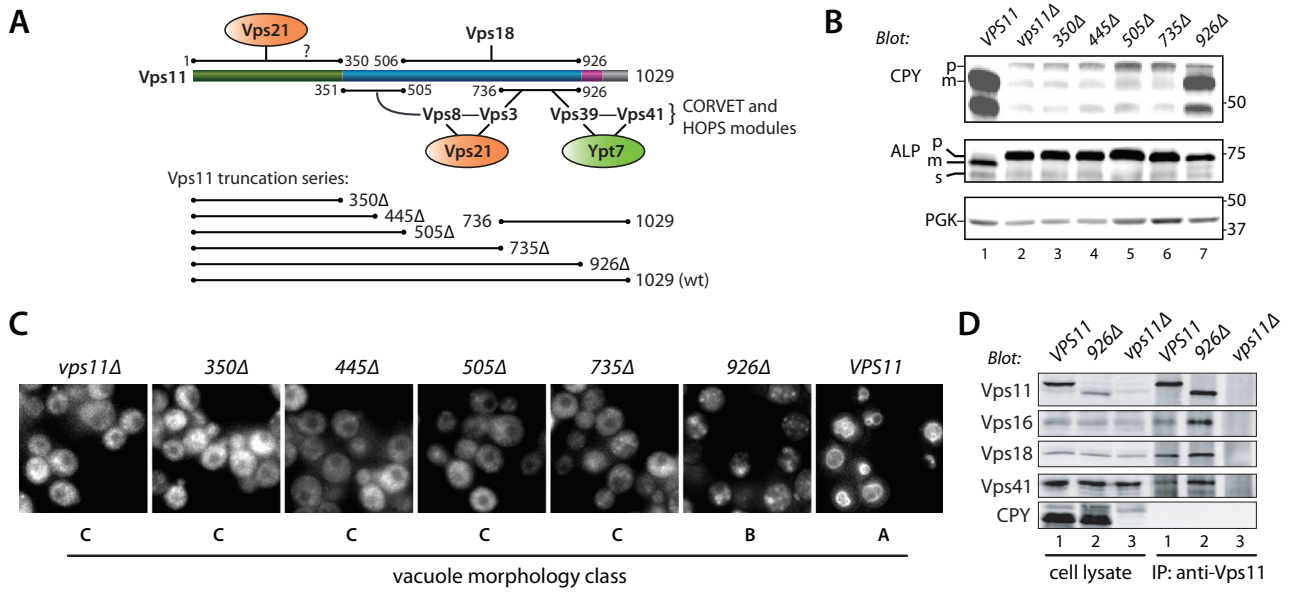

FIGURE 7: Multiple functional domains reside within the Vps11 CTD. (A) Map of Vps11 interactions. The cartoon shows Vps11 interactions and a summary of the Vps11 truncation series. (B) CPY and ALP maturation phenotypes of cells harboring C-terminally truncated forms of Vps11. Accumulation of pro (p) forms of CPY and ALP indicate trafficking defects. (C) Vacuole morphology of *vps11* truncation mutants. Vacuoles were stained with the vital fluorescent dye FM4–64 by pulse-chase labeling. (D) Coimmunoprecipitation reveals an intact HOPS complex in *vps11–926* cells. Lysates of the indicated mutant cells were immunoprecipitated with Vps11 antibodies under nondenaturing conditions, and the eluates were analyzed by immunoblotting. Cell lysate lanes contain 10% load relative to the immunoprecipitation eluate.

reported to be a Ypt7 GEF (Wurmser *et al.*, 2000; Binda *et al.*, 2009). Vps41 binds Ypt7-GTP directly (Figure 3B), which explains why Vps41 is essential for stable binding of the HOPS holocomplex to Ypt7-GTP (Brett *et al.*, 2008). However, although Vps39 shows a lack of nucleotide specificity in Ypt7 binding, as might be expected for a GEF, highly purified preparations of Vps39 or Vps39–860Δ failed to exhibit any nucleotide exchange activity in fluorescence and radioisotopic assays that readily detected the activities of bona fide GEFs (Nordmann *et al.*, 2010; Ostrowicz *et al.*, 2010; Lobingier, Brett, and Merz, unpublished results). Instead, the major Ypt7 GEF activity appears to reside within the Ccz1/Mon1 complex (Kucharczyk *et al.*, 2000; 2001; Nordmann *et al.*, 2010). The Vps39 CTD is dispensable for Vps39 binding to Ypt7 and Vps41 (Figures 1 and 2D; Supplemental Table S2), and for binding of HOPS to Ypt7-GTPγS (Brett and Merz, unpublished results). The Vps39 CTD is, however, essential for Vps39 function in vivo, because its deletion phenocopies a *vps39*Δ null mutant (Figure 4 and Supplemental Table S2; Wurmser *et al.*, 2000).

Like Vps39 and Vps41, the CORVET subunits Vps3 and Vps8 function as a Rab-recognition module that signals through Vps11. As with Vps39, the Vps3 CTD binds the Vps11 CTD, and this domain is needed for Vps3 function. In Y2H analyses we identified Vps21-interacting domains in both Vps3 and Vps8. While this manuscript was in preparation, Y2H hits between Vps8 and Vps21 were reported by two other groups (Markgraf *et al.*, 2009; Pawelec *et al.*, 2010). Moreover, we obtained genetic data, using the *VPS8–200* suppressor of *vps11–445*Δ, that Vps8 and Vps21 functionally interact. In our Y2H analyses, both Vps8 and Vps8–200 exhibited a preference for Vps21-GTP. In our experiments, Vps3 always exhibited preferential binding to activated Vps21. Native Vps3, as a CORVET substituent, is selectively retained on Vps21-GTP (Figure 4C). Using purified proteins we demonstrated that Vps3 binds Vps21-GTPγS directly (Figure 4D). In contrast, recent work suggested that Vps3 contributes to GDP-selective Vps21 binding by the CORVET holocomplex, and it was proposed in this work that Vps3 might function as a Vps21 GEF (Peplowska *et al.*, 2007). However, as with Vps39, we have been unable to detect any nucleotide exchange activity mediated by purified Vps3 using assays that readily detect exchange mediated by a bona fide Vps21 GEF, Vps9 (Lobingier, Brett, and Merz, unpublished results). While this article was under revision, similar results for Vps3 were reported by Ostrowicz *et al.* (2010).

The distinct nucleotide specificities of the Rab-recognition modules within CORVET and HOPS are particularly striking. The CORVET subunits Vps3 and Vps8 appear to simply search for the presence or absence of Vps21-GTP. In contrast, the HOPS Rab-recognition module contains one subunit, Vps41, that detects Ypt7-GTP and a second subunit, Vps39, that is insensitive to the nucleotide binding state of Ypt7. HOPS might therefore monitor not only the presence of Ypt7-GTP but also the *ratio* of Ypt7-GTP to Ypt7 GDP. The functional consequences of the divergent Rab-binding modalities of HOPS and CORVET are not yet understood.

As membrane traffic traverses successive endolysosomal organelles, the Rab5 orthologue Vps21 is replaced by the Rab7 orthologue Ypt7 (Figure 9). CORVET and HOPS, operating in concert with the GEFs Vps9 and Ccz1-Mon1, appear to control this Rab cascade (Rink *et al.*, 2005; Vonderheit and Helenius, 2005; Peplowska *et al.*, 2007). Vps11 appears to be a central scaffold upon which both HOPS and CORVET assemble. Deletion analyses of Vps11 (Figure 5 and Supplemental Table S2) confirm the functional importance of the Vps11 CTD. The almost complete functional complementation in trans of two Vps11 truncation mutants (–735Δ and –926Δ) by a C-terminal (736–1029) fragment of Vps11—which contains a binding site or sites for the C-termini of Vps3 and Vps39—underscores the modularity of this region. Vps11 may be a simple structural scaffold or it could have a more dynamic role in linking Rab signaling to Vps-C outputs, including the SNARE machinery that mediates fusion at the endosome and vacuole. In either case, the Vps11 CTD is now the prime candidate for the location at

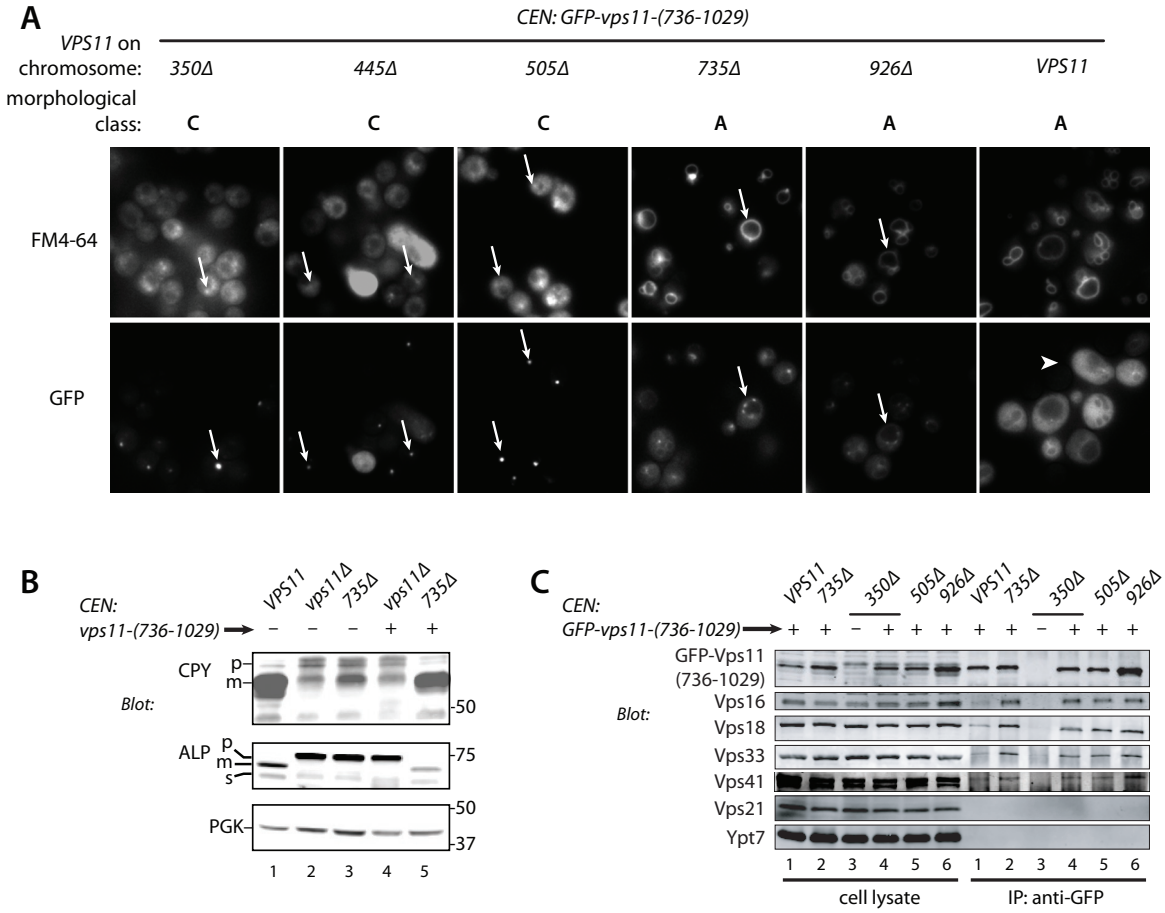

FIGURE 8: Split Vps11 expressed as N- and C-terminal fragments is functional. (A) Vacuole morphology of *vps11* truncation mutants coexpressing GFP-Vps11-(736–1029). Top row, vacuoles were stained with the vital fluorescent dye FM4–64 by pulse-chase labeling. Bottom row, the localization of GFP-Vps11-(736–1029) in the same cells is also shown. GFP-Vps11-(736–1029) localizes to puncta in Vps11–350Δ, –445Δ, and –505Δ mutant cells and at the vacuole rim in the Vps11–735Δ and –926Δ mutant cells (arrows). In contrast, GFP-Vps11-(736–1029) localizes to the cytoplasm in cells containing full-length Vps11 (arrowhead). (B) CPY and ALP maturation in Vps11 truncation mutants coexpressing GFP-Vps11-(736–1029). Note rescue of the 735Δ mutant (lane 5). (C) Coimmunoprecipitation of HOPS subunits with GFP-Vps11-(736–1029). Lysates from the indicated mutants, with or without GFP-Vps11-(736–1029) expression, were immunoprecipitated with anti-GFP. Cell lysate lanes contain 10% load relative to IP eluate. Note that HOPS subunits copurify with low efficiency when full-length Vps11 is present (lanes 1). No HOPS subunits copurify when GFP-Vps11-(736–1029) is not expressed (lanes 3).

which switching between the HOPS and CORVET Vps-C configurations might occur. Consistent with the idea that the Vps11 CTD is a key element in this cascade, the C-terminal RING domain of Vps11 appears to function predominantly in fusion at the vacuole (Figure 7 and Supplemental Table S4). Moreover, we recently isolated new *vps11* alleles bearing mutations solely in the Vps11 CTD and exhibiting selective defects in traffic through late endosomes, to the vacuole, or both (Nickerson, Fawcett, and Merz, unpublished results). We are now working to understand how Rab signaling through Vps-C complexes drives fusion and other "output" processes (Nickerson *et al.*, 2009) and how Vps-C complexes signal in time and space to transport cargoes derived from early endosomes, the late Golgi, autophagosomes, and cytoplasm-to-vacuole transport (CVT) vesicles through the endolysosomal system.

MATERIALS AND METHODS

Strains and plasmids

Yeast strains used are described in Supplemental Table 1. Plasmids for Y2H screening are listed in Supplemental Tables S2 and S3. Plasmids were constructed either by conventional cloning or by gap-repair methods.

Y2H assays

Two-hybrid vectors were constructed using gap-repair and homologous recombination (Uetz *et al.*, 2000). Prey domains were cloned into the plasmid pOAD and transformed into the yeast strain PJ-9-4a. Bait domains were cloned into pOBD-2 and transformed into PJ69-4α. Clonal isolates were obtained and verified by PCR and in many cases by DNA sequencing. Interaction tests were performed by mating haploid strains containing the bait and prey vectors. Liquid cultures of the bait and prey strains were grown in selective media then mixed in 96-well plates and pinned to YPD (yeast extract peptone dextrose) plates supplemented with adenine using a 48-spoke inoculating manifold. The mating plates were grown at 30°C overnight, then diploid cells were selected by replica plating onto medium lacking tryptophan and leucine and supplemented with adenine. Diploid colonies were grown at 30°C for 2 d, then tested for Y2H interactions by replica plating to medium lacking

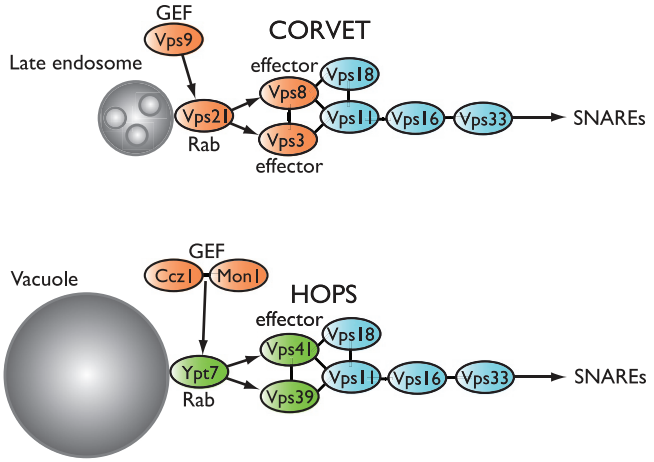

FIGURE 9: Interactions of HOPS and CORVET subunits with one another and with cognate Rabs. The subunit interaction topology summarized in this diagram integrates both biochemical and Y2H data. The similar diagram in Figure 1 summarizes only Y2H interactions.

tryptophan, leucine, and histidine, supplemented with adenine and various concentrations of 3-amino-1,2,4-triazole (3-AT), ranging from 1.5 to 25 mM. The use of low-copy vectors (pOAD and pOBD-2), and the assay of histidine auxotrophy in the presence of 3-AT at >1 mM, together almost totally suppresses false-positive signals in Y2H experiments (Braun *et al.*, 2009; Chen *et al.*, 2010). After 5 d at 30°C, plates were scored for growth. Bait–prey interactions were scored as follows: very strong (3), strong (2), weak (1), or none (0). Mean scores are presented; in a large majority of cases these mean scores represent results from two or three independent interaction tests. In many cases, positive hits from the Y2H surveys were also subjected to further rounds of screening, which are not reflected in the survey scores presented in Supplemental Tables S2 and S3.

Protein purification

His_6- and GST-fused Vps-C subunits were expressed in BTI-Tn-5B1–4 (High-5) insect cells as described (Brett *et al.*, 2008). Baculovirus vectors were constructed and propagated using the Bac-to-Bac system as recommended by the vendor (Invitrogen, Carlsbad, CA). Suspension-adapted or monolayer insect cells were infected with passage-3 or passage-4 virus, grown for 3 d at 27°C, and harvested. All subsequent steps were performed at 4°C or on ice. Cells were resuspended in lysis buffer (50 mM HEPES [4-(2-hydroxyethyl)-1-piperazineethanesulfonic acid], 400 mM NaCl, 5 mM 2-mercaptoethanol, 10% glycerol, 0.5% Triton X-100, supplemented with pH 7.8, 400 µM phenylmethylsulfonyl fluoride, 1 µg/ml leupeptin, 1 µg/ml pepstatin, 100 µM Pefabloc SC [Roche, Mannheim, Germany], and 20 mM imidazole). The cells were lysed with detergent and brief sonication, and the lysate was clarified by centrifugation (18,000 × *g*, 25 min). Clarified lysates were incubated with glutathione sepharose 4B (GE Heathcare, Piscataway, NJ) for 2 h, and resin was subsequently washed three times with the lysis buffer and eluted with lysis buffer supplemented with 10 mM reduced glutathione. GST eluates were then incubated with preequilibrated Ni^{2+}-NTA resin (GE Healthcare) for 1 h, washed three times with lysis buffer supplemented with 35 mM imidazole, eluted with lysis buffer supplemented with 500 mM imidazole, and analyzed by SDS–PAGE.

Rab pulldowns

GST-Rab fusion proteins were cloned, expressed, and purified as described (Brett *et al.*, 2008). Nucleotide loading of Rab proteins was performed either (procedure 1) as described (Brett *et al.*, 2008) or (procedure 2) by washing the resin once with nucleotide loading buffer (50 mM Tris, 200 mM NaCl, 7.5 mM EDTA, 5 mM 2-mercaptoethanol, pH 8.0), then incubating the resin with the nucleotide loading buffer and 20-fold molar exess of nucleotide for 2 h at room temperature. The reaction was terminated with an excess of quenching buffer (50 mM Tris, 200 mM NaCl, 15 mM $MgCl_2$, 5 mM, pH 8.0). The resin was washed three times with reaction buffer (50 mM Tris, 200 mM NaCl, 5 mM $MgCl_2$, 5 mM 2-mercaptoethanol, pH 8.0). Cell lysates or purified Vps-C subunits were incubated with the resin in reaction buffer for 1 h at 4°C, and the resin was then washed with reaction buffer three times. Bound protein was eluted from the beads in reaction buffer supplemented with 10 mM reduced glutathione, pH 8.0 (final), and the eluates were analyzed by SDS–PAGE.

Immunoprecipitation

Cell lysates were prepared, and immunoprecipitations were performed as described (Angers and Merz, 2009).

Protein sorting and vacuole morphology

Mutant yeast strains were propagated at room temperature to minimize selection for suppressor mutations. Liquid cultures were grown to log phase (OD_{600} = 0.6–1.0) in complex or synthetic media at 26°C. Cell pellets were chilled on ice and washed in 10 mM NaN_3. Washed pellets were resuspended in 40 µl SDS–PAGE sample buffer per 1 ml × OD_{600}. After addition of sterile glass beads, samples were boiled 15 min and vortexed 3 min. Western blots were probed using monoclonal mouse antibodies against CPY, ALP, and PGK (phosphoglycerate kinase, Pgk1) (all from Invitrogen) and analyzed with a LICOR (Lincoln, NE) Odyssey fluorescence scanner. Colorimetric assays to detect secretion of CPY-invertase were performed as described previously (Darsow *et al.*, 2000). Vacuole morphology was evaluated by pulse-chase labeling with the endocytic tracer FM4–64 (Invitrogen) as described (Brett *et al.*, 2008). Subcellular fractionation by differential centrifugation was performed as described (Angers and Merz, 2009) Fluorescence microscopic analysis of GFP-CPS localization in FM4–64-labeled cells used the plasmid pGO47 (Odorizzi *et al.*, 1998).

ACKNOWLEDGMENTS

We thank R. Gardner for generous assistance with mass spectrometry; E. Jones, C. Woolford, S. Emr, B. Horazdovsky, G. Odorizzi, and W. Wickner for strains and reagents; C. Ungermann for discussion of unpublished results; and S. Fields and M. Vignali for invaluable advice on setting up large-scale Y2H screens. Our work is funded by NIH-NIGMS GM077349. B.T.L., C.G.A., and A.P. were supported by NIH-NIGMS T32 GM07270, and D.S. by an HHMI Undergraduate Research Fellowship. A.J.M. is a Research Scholar, and D.P.N is a Postdoctoral Fellow, of the American Cancer Society.

REFERENCES

Angers CG, Merz AJ (2009). HOPS interacts with Apl5 at the vacuole membrane and is required for consumption of AP-3 transport vesicles. Mol Biol Cell 20, 4563–4574.

Binda M, Peli-Gulli MP, Bonfils G, Panchaud N, Urban J, Sturgill TW, Loewith R, De Virgilio C (2009). The Vam6 GEF controls TORC1 by activating the EGO complex. Mol Cell 35, 563–573.

Braun P *et al.* (2009). An experimentally derived confidence score for binary protein–protein interactions. Nat Methods 6, 91–97.

Brett CL, Plemel RL, Lobinger BT, Vignali M, Fields S, Merz AJ (2008). Efficient termination of vacuolar Rab GTPase signaling requires coordinated action by a GAP and a protein kinase. J Cell Biol 182, 1141–1151.
Chen YC, Rajagopala SV, Stellberger T, Uetz P (2010). Exhaustive benchmarking of the yeast two-hybrid system. Nat Methods 7, 667–668 author reply 668.
Chivian D, Kim DE, Malmstrom L, Schonbrun J, Rohl CA, Baker D (2005). Prediction of CASP-6 structures using automated Robetta protocols. Proteins 61 Suppl 7, 193–200.
Conibear E, Stevens TH (1998). Multiple sorting pathways between the late Golgi and the vacuole in yeast. Biochim Biophys Acta 1404, 211–230.
Darsow T, Odorizzi G, Emr SD (2000). Invertase fusion proteins for analysis of protein trafficking in yeast. Methods Enzymol 327, 95–106.
Grosshans BL, Ortiz D, Novick P (2006). Rabs and their effectors: achieving specificity in membrane traffic. Proc Natl Acad Sci USA 103, 11821–11827.
Hama H, Tall GG, Horazdovsky BF (1999). Vps9p is a guanine nucleotide exchange factor involved in vesicle-mediated vacuolar protein transport. J Biol Chem 274, 15284–15291.
Horazdovsky BF, Cowles CR, Mustol P, Holmes M, Emr SD (1996). A novel RING finger protein, Vps8p, functionally interacts with the small GTPase, Vps21p, to facilitate soluble vacuolar protein localization. J Biol Chem 271, 33607–33615.
Kim DE, Chivian D, Baker D (2004). Protein structure prediction and analysis using the Robetta server. Nucleic Acids Res 32, W526–W531.
Kinchen JM, Ravichandran KS (2010). Identification of two evolutionarily conserved genes regulating processing of engulfed apoptotic cells. Nature 464, 778–782.
Kucharczyk R, Dupre S, Avaro S, Haguenauer-Tsapis R, Slonimski PP, Rytka J (2000). The novel protein Ccz1p required for vacuolar assembly in *S. cerevisiae* functions in the same transport pathway as Ypt7p. J Cell Sci 113, pt 23), 4301–4311.
Kucharczyk R, Hoffman-Sommer M, Piekarska I, von Mollard GF, Rytka J (2009). The *S. cerevisiae* protein Ccz1p interacts with components of the endosomal fusion machinery. FEMS Yeast Res 9, 565–573.
Kucharczyk R, Kierzek AM, Slonimski PP, Rytka J (2001). The Ccz1 protein interacts with Ypt7 GTPase during fusion of multiple transport intermediates with the vacuole in *S. cerevisiae*. J Cell Sci 114, 3137–3145.
Markgraf DF, Ahnert F, Arlt H, Mari M, Peplowska K, Epp N, Griffith J, Reggiori F, Ungermann C (2009). The CORVET subunit Vps8 cooperates with the Rab5 homolog Vps21 to induce clustering of late endosomal compartments. Mol Biol Cell 20, 5276–5289.
Mima J, Hickey CM, Xu H, Jun Y, Wickner W (2008). Reconstituted membrane fusion requires regulatory lipids, SNAREs and synergistic SNARE chaperones. EMBO J 27, 2031–2042.
Nakamura N, Hirata A, Ohsumi Y, Wada Y (1997). Vam2/Vps41p and Vam6/Vps39p are components of a protein complex on the vacuolar membranes and involved in the vacuolar assembly in the yeast *S. cerevisiae*. J Biol Chem 272, 11344–11349.
Nickerson DP, Brett CL, Merz AJ (2009). Vps-C complexes: gatekeepers of endolysosomal traffic. Curr Opin Cell Biol 21, 543–551.
Nordmann M, Cabrera M, Perz A, Brocker C, Ostrowicz C, Engelbrecht-Vandre S, Ungermann C (2010). The Mon1-Ccz1 complex is the GEF of the late endosomal Rab7 homolog Ypt7. Curr Biol 20, 1654–1659.
Odorizzi G, Babst M, Emr SD (1998). Fab1p PtdIns(3)P 5-kinase function essential for protein sorting in the multivesicular body. Cell 95, 847–858.
Ostrowicz CW, Brocker C, Ahnert F, Nordmann M, Lachmann J, Peplowska K, Perz A, Auffarth K, Engelbrecht-Vandre S, Ungermann C (2010). Defined subunit arrangement and Rab interactions are required for functionality of the HOPS tethering complex. Traffic 11, 1334–1346.
Pawelec A, Arsic J, Kolling R (2010). Mapping of Vps21 and HOPS binding sites in Vps8 and effect of binding site mutants on endocytic trafficking. Eukaryot Cell 9, 602–610
Peplowska K, Markgraf DF, Ostrowicz CW, Bange G, Ungermann C (2007). The CORVET tethering complex interacts with the yeast Rab5 homolog Vps21 and is involved in endo-lysosomal biogenesis. Dev Cell 12, 739–750.
Peterson MR, Burd CG, Emr SD (1999). Vac1p coordinates Rab and phosphatidylinositol 3-kinase signaling in Vps45p-dependent vesicle docking/fusion at the endosome. Curr Biol 9, 159–162.
Peterson MR, Emr SD (2001). The class C Vps complex functions at multiple stages of the vacuolar transport pathway. Traffic 2, 476–486.
Poteryaev D, Datta S, Ackema K, Zerial M, Spang A (2010). Identification of the switch in early-to-late endosome transition. Cell 141, 497–508.
Price A, Seals D, Wickner W, Ungermann C (2000). The docking stage of yeast vacuole fusion requires the transfer of proteins from a *cis*-SNARE complex to a Rab/Ypt protein. J Cell Biol 148, 1231–1238.
Pulipparacharuvil S, Akbar MA, Ray S, Sevrioukov EA, Haberman AS, Rohrer J, Kramer H (2005). *Drosophila* Vps16A is required for trafficking to lysosomes and biogenesis of pigment granules. J Cell Sci 118, 3663–3673.
Raymond CK, O'Hara PJ, Eichinger G, Rothman JH, Stevens TH (1990). Molecular analysis of the yeast VPS3 gene and the role of its product in vacuolar protein sorting and vacuolar segregation during the cell cycle. J Cell Biol 111, 877–892.
Rehling P, Darsow T, Katzmann DJ, Emr SD (1999). Formation of AP-3 transport intermediates requires Vps41 function. Nat Cell Biol 1, 346–353.
Rieder SE, Emr SD (1997). A novel RING finger protein complex essential for a late step in protein transport to the yeast vacuole. Mol Biol Cell 8, 2307–2327.
Rink J, Ghigo E, Kalaidzidis Y, Zerial M (2005). Rab conversion as a mechanism of progression from early to late endosomes. Cell 122, 735–749.
Sato TK, Rehling P, Peterson MR, Emr SD (2000). Class C Vps protein complex regulates vacuolar SNARE pairing and is required for vesicle docking/fusion. Mol Cell 6, 661–671.
Seals DF, Eitzen G, Margolis N, Wickner WT, Price A (2000). A Ypt/Rab effector complex containing the Sec1 homolog Vps33p is required for homotypic vacuole fusion. Proc Natl Acad Sci USA 97, 9402–9407.
Sevrioukov EA, He JP, Moghrabi N, Sunio A, Kramer H (1999). A role for the deep orange and carnation eye color genes in lysosomal delivery in *Drosophila*. Mol Cell 4, 479–486.
Srivastava A, Woolford CA, Jones EW (2000). Pep3p/Pep5p complex: a putative docking factor at multiple steps of vesicular transport to the vacuole of *S. cerevisiae*. Genetics 156, 105–122.
Stroupe C, Collins KM, Fratti RA, Wickner W (2006). Purification of active HOPS complex reveals its affinities for phosphoinositides and the SNARE Vam7p. EMBO J 25, 1579–1589.
Sudhof TC, Rothman JE (2009). Membrane fusion: grappling with SNARE and SM proteins. Science 323, 474–477.
Uetz P *et al*. (2000). A comprehensive analysis of protein-protein interactions in *S. cerevisiae*. Nature 403, 623–627.
Venkatesan K *et al*. (2009). An empirical framework for binary interactome mapping. Nat Methods 6, 83–90.
Vonderheit A, Helenius A (2005). Rab7 associates with early endosomes to mediate sorting and transport of Semliki forest virus to late endosomes. PLoS Biol 3, e233.
Wang CW, Stromhaug PE, Kauffman EJ, Weisman LS, Klionsky DJ (2003). Yeast homotypic vacuole fusion requires the Ccz1-Mon1 complex during the tethering/docking stage. J Cell Biol 163, 973–985.
Wang CW, Stromhaug PE, Shima J, Klionsky DJ (2002). The Ccz1-Mon1 protein complex is required for the late step of multiple vacuole delivery pathways. J Biol Chem 277, 47917–47927.
Woolford CA, Bounoutas GS, Frew SE, Jones EW (1998). Genetic interaction with Vps8–200 allows partial suppression of the vestigial vacuole phenotype caused by a Pep5 mutation in *S. cerevisiae*. Genetics 148, 71–83.
Wurmser AE, Sato TK, Emr SD (2000). New component of the vacuolar class C-Vps complex couples nucleotide exchange on the Ypt7 GTPase to SNARE-dependent docking and fusion. J Cell Biol 151, 551–562.
Ybe JA, Brodsky FM, Hofmann K, Lin K, Liu SH, Chen L, Earnest TN, Fletterick RJ, Hwang PK (1999). Clathrin self-assembly is mediated by a tandemly repeated superhelix. Nature 399, 371–375.

Figure S1

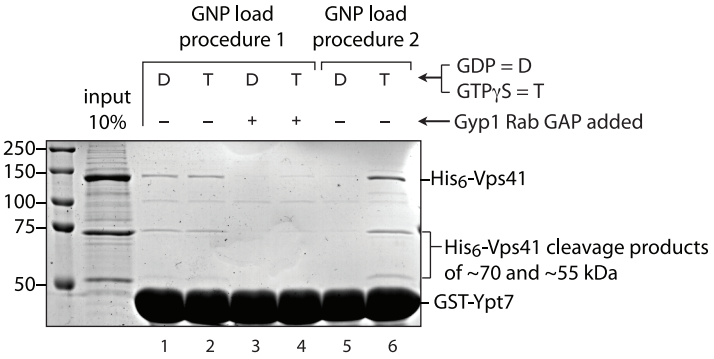

Figure S2

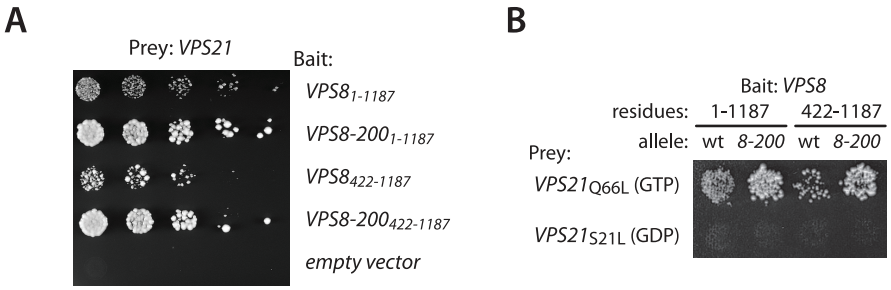

Supplementary Table 1. Informatic analyses: domain structures of of Vps-C/HOPS and Vps-C/CORVET subunits from *Saccharomyces cerevisiae* and *Homo sapiens*

Protein	Ref/Systemat	Length	FW	DomStart	DomEnd	Method	Fold/motif	Model	ModStart	ModEnd	RawSig	AdjSig
Vps3	YDR495C	1011	117	1	140	Ginzu/msa						
				141	238	Ginzu/cutpref						
				329	416	Ginzu/msa						
				417	636	Ginzu/cutpref						
				637	853	Ginzu/cutpref						
				854	996	Ginzu/cutpref						
Vps8	YAL002W	1274	145									
				122	161	SMART	WD40				2.30E-01	0.6
				181	224	SMART	WD40				8.70E+01	-1.9
				1198	1265	SMART	RING				1.60E-02	1.8
				125	161	pfam motif scan	WD40				8.40E-01	0.1
				484	664	pfam motif scan	Clathrin				5.70E-01	0.2
				1001	1023	pfam motif scan	Vps16_C				3.00E-01	0.5
				1197	1268	pfam motif scan	PHD				2.40E-01	0.6
				1231	1265	pfam motif scan	zf-C4HC4				6.20E-02	1.2
				508	665	Ybe et al.	Clathrin (1 of 2)					
				915	1092	Ybe et al.	Clathrin (2 of 2)					
				1	399	Manual/pdbblast	B-propellor	1NR0A Aip1p ortholog	151	529	3.11E+01	31.1
				1	421	Ginzu/pdbblast	B-propellor	1NR0A Aip1p ortholog	151	557	3.52E+01	35.2
				422	722	Manual/Ginzu/3djury	A-solenoid	1BK5a Srp1p karyopherin alpha	1	359	1.02E+00	1.0
				723	1187	Ginzu/pdbblast	A-solenoid	1B89a Clathrin proximal leg	25	443	2.45E+01	24.5
				1188	1274	Ginzu/ffas03		1V87a RING finger from mouse Deltex 2	5	95	2.45E+00	2.5
Vps11/Pep5p	YMR231W	1029	117.5									
				882	913	SMART	coiled-coil					
				927	973	SMART	PHD					
				928	972	SMART	RING					
				373	432	pfam motif scan					3.20E-03	2.5
				406	555	pfam motif scan	pre:CLATHRIN_REPEAT				2.50E-05	4.6
				928	972	pfam motif scan	prf:ZF_RING_2				1.10E-03	3.0
				943	975	pfam motif scan	pfam_fs:PHD				1.60E-06	5.8
				928	972	pfam motif scan	pfam_fs:zf-C3HC4				5.50E-04	3.3
				927	975	pfam motif scan	pfam_ls:PHD				2.10E-04	3.7
				928	972	pfam motif scan	pfam_ls:zf-C3HC4				4.10E-04	3.4
				460	583	Ybe et al.	Clathrin					
				364	505	Ginzu/pdbblast	A-bundle	1NA0a engineered TPR A-helix array	50	105	3.52E+00	3.5

				506	925	Ginzu/3Djury	A-solenoid	1EJLI Mouse importin alpha	8	391	2.07E+00	2.1
				1	350	Manual/pdbblast	B-propellor	1GG2b G-beta			3.94E+01	39.4
				926	C	Manual/pdbblast	RING C3HC4	1JM7b Brca1BARD1 RING			4.00E+00	4.0
				1	349	Manual	B-propellor					
				350	926	Manual	A-solenoid					
				926	1029	Manual	RING					
hVPS11	Q9H270	941	107.8									
				822	860	SMART	RING				6.00E-05	4.2
				822	860	pfam motif scan	zf-C3HC4				2.10E-03	2.7
				1	72	Ginzu/pdbblast		1P22a Beta-TrCP1 WD40 domain	143	159	4.24E+01	42.4
				73	337	Ginzu/pdbblast		1PI6a yeast AIp1p	55	304	1.42E+01	14.2
				338	715	Ginzu/pdbblast	A-solenoid	1B89a Clathrin proximal leg	133	449	3.11E+01	31.1
				716	941	Ginzu/pdbblast		1FBVa c-Cbl SH2-like and RING domains	235	378	5.00E+00	5.0
				716	861	Ginzu/pdbblast		1FBVa c-Cbl SH2-like and RING domains	235	378	5.00E+00	5.0
				862	941	Ginzu/3Djury		1SFFa Gamma-Aminobutyrate Aminotrans	313	381	1.02E+00	1.0
Vps16p	YPL045W	798	92.7									
				4	379	SMART	pfam:VPS16N				8.00E-216	215.1
				478	798	SMART	pfam:VPS16C				1.60E-193	192.8
				4	379	pfam motif scan	pfam_fs:Vps16_N				6.60E-218	217.2
				478	798	pfam motif scan	pfam_fs:Vps16_C				1.40E-193	192.9
				1	395	Ginzu/ffas03	B-propellor	1TYQc p40 of Arp2/3 complex	1	372	2.18E+00	2.2
				1	530	Ginzu/ffas03	B-propellor	1NR0A Aip1p ortholog	74	606	2.30E+00	2.3
				396	798	Ginzu/3Djury	A-solenoid/bundle	1N1Ba bornyl diphosphate synthase	62	489	2.06E+00	2.1
				531	798	Ginzu/3Djury	A-solenoid	1IB2a Pumilio-1 PUM repeat	26	296	2.06E+00	2.1
				1	285	Manual/3Djury	B-propellor	1GOTb Transducin beta	25	331	4.91E+00	4.9
				1	308	Manual/ffas03	B-propellor	1ERJa Tup1 WD40 domain	36	392	4.95E+00	5.0
				285	798	Manual/3Djury	A-solenoid	1EE4a Srp1p karyopherin alpha			2.05E+00	2.0
				1	307	Manual	B-propellor					
				308	798	Manual	B-propellor					
hVPS16	Q9H269	839	94.6									
				4	420	SMART	pfam:Vps16_N				4.60E-270	270.0
				517	835	SMART	pfam:Vps16_N				2.10E-202	202.0
				4	420	pfam motif scan	pfam_fs:Vps16_N				3.50E-271	270.5
				517	835	pfam motif scan	pfam_fs:Vps16_C				1.60E-203	202.8

				1	568	Ginzu/ffas03	B-propellor/A-solenoid	1NR0A Aip1p ortholog	1	553	2.61E+00	2.6
				569	839	Ginzu/3Djury	A-solenoid	1OYZa E. coli YibA	5	280	1.55E+00	1.6
Vps18/Pep3p	**YLR148W**	**918**	**107.4**									
				214	380	SMART	pfam:Pep3_Vps18				2.30E-85	84.6
				585	741	SMART	CLH				1.60E-27	26.8
				826	894	SMART	RING				4.50E-01	0.3
				214	380	pfam motif scan	pfam_fs:Pep3_Vps18				2.00E-87	86.7
				585	741	pfam motif scan	pre:CLATHRIN_REPEAT				2.40E-02	1.6
				585	741	pfam motif scan					6.80E-29	28.2
				585	741	pfam motif scan	pfam_ls:Clathrin				7.20E-29	28.1
				770	785	pfam motif scan	pfam_fs:Merozoite_SPAM				7.30E-05	4.1
				585	741	Ybe et al.	Clathrin					
				1	337	Ginzu/pdbblast	B-propellor	1ERJa Tup1 WD40 domain	55	387	3.97E+01	39.7
				338	733	Ginzu/pdbblast	A-solenoid	1B89a Clathrin proximal leg	116	449	3.80E+01	38.0
				734	917	Ginzu/cutpref					na	
hVPS18	**Q9P253**	**973**	**110.1**									
				291	436	SMART	pfam:Pep3_Vps18				3.60E-75	74.4
				291	436	pfam motif scan	pfam:Pep3_Vps18				2.70E-76	75.6
				618	772	pfam motif scan	Clathrin				5.10E-03	2.3
				1	515	Ginzu/pdbblast	B-propellor	1BPOa Clathrin N-term and linker	3	471	9.40E+01	94.0
				516	743	Ginzu/pdbblast	A-solenoid	1B89a Clathrin proximal leg	268	449	4.21E+01	42.1
				744	973	Ginzu/msa					3.37E+00	3.4
Vps39/Vam6p	**YDL077C**	**886**	**1049**									
				na	na	SMART	none recognized					
				642	670	pfam motif scan	pfam:fs:PPR				6.20E-03	2.2
				730	896	Ybe et al.	Clathrin					
				596	715	Manual; Ref 1	"domain I"				na	
				733	893	Manual; Ref 1	Clathrin				na	
				905	1021	Manual; Ref 1	"domain II"				na	
				1	434	Ginzu/3Djury	B-propellor	1NEXb Ubiquitin ligase	1	430	2.07E+00	2.1
				435	860	Manual/Ginzu/pdbbla	A-solenoid	1B89a Clathrin proximal leg	84	449	5.31E+01	53.1
				431	870	Manual/Ginzu/3Djury	A-solenoid	1QGKa Importin beta	50	470	2.55E+00	2.6
				547	860	Manual/Ginzu/pdbbla	A-solenoid	1B89a Clathrin proximal leg	207	449	2.40E+00	2.4

				861	979	Ginzu/3Djury		1A17 Prot Pi'ase 5 TTR repeats	38	154	1.01E+00	1.0
				861	979	Ginzu/3Djury		1SQBa bcl, M16_peptidase domain	55	178	1.65E+00	1.7
				980	1049	Ginzu/pdbblast	RING-like	1IYMa Ring-H2 finger of E15	434	503	4.00E+00	4.0
				980	1049	Ginzu/msa					1.11E+01	11.1
				1	444	Manual	B-propellor				na	
				445	893	Manual	A-solenoid				na	
				894	980	Manual	A-helical/unstructured				na	
				980	1049	Manual	RING-like				na	
				610	705	Searchwise (Ref2]	Clathrin Linker/alpha-COP	Clathrin Linker/alpha-COP			na	
hVam6	**Q96JC1**											
				10	300	SMART	CNH [citron]				1.34E-03	2.9
NOTE: hVps39 appears to be a												
srtuctural and functional homolog				15	294	pfam motif scan	pfam:lsCNH [citron]				1.50E-10	9.8
of yeast Vps3p, **not** Vps39p.				15	186	pfam motif scan	pfam:fsCNH [citron]				2.10E-04	3.7
				217	272	pfam motif scan	pre:ROM_MOTIF				1.00E-02	2.0
				281	306	pfam motif scan	pfam_fs:NHL				2.70E-03	2.6
				481	532	pfam motif scan	pfam_Fs:Clathrin				2.00E-04	3.7
				1	271	Ginzu:3Djury	B-propellor	1ERJa Tup1 WD40 domain	92	384	4.98E+00	5.0
				272	687	Ginzu/pdbblast	A-solenoid	1B89a Clathrin proximal leg	28	449	3.01E+01	30.1
				688	886	Ginzu:3Djury		1NAQa E. coli Cut1	12	119	2.06E+00	2.1
Vps41/Vam2	**YDR080W**	**992**	**113.4**									
				144	181	SMART	WD-40				2.30E-03	2.6
				184	225	SMART	WD-40				3.20E+01	-1.5
				753	901	SMART	CLH				2.90E-42	41.5
				753	901	Ybe et al.	Clathrin					
				146	181	pfam motif scan	pfam_fs:WD40				9.50E-08	7.0
				146	181	pfam motif scan	pfam_ls:WD40				4.80E-05	4.3
				753	901	pfam motif scan	pre:CLATHRIN_REPEAT				2.40E-19	18.6
				753	901	pfam motif scan	pfam_fs:Clathrin				2.30E-38	37.6
				753	901	pfam motif scan	pfam_ls:Clathrin				6.00E-39	38.2
				1	96	Ginzu/pdbblast	B-propellor	1ERJa Tup1 WD40 domain	63	115	4.37E+01	43.7
				97	468	Ginzu/pdbblast	B-propellor	1P22a Beta-TrCP1 WD40 domain	138	415	4.73E+01	47.3
				469	992	Ginzu/ffas03	A-solenoid	1B89a Clathrin proximal leg	1	416	2.06E+00	2.1
				1	501	Manual/Ginzu2	B-propellor				na	
				806	903	Searchwise (Ref2]	Clathrin Linker/alpha-COP	Clathrin Linker/alpha-COP			na	
hVPS41	**gi2506924**											
				571	712	SMART	CLH				1.90E-42	41.7

				791	838	SMART	RING					7.60E-02	1.1
				75	112	pfam motif scan	pfam_fs:WD40					3.90E-03	2.4
				571	712	pfam motif scan	pre:CLATHRIN_REPEAT					9.70E-22	21.0
				571	712	pfam motif scan	pfam_fs:Clathrin					1.90E-07	6.7
				571	712	pfam motif scan	pfam_ls:Clathrin					8.00E-07	6.1
				791	839	pfam motif scan	prf:ZF_RING_2					1.30E-02	1.9
				1	329	Ginzu/pdbblast	B-propellor	1P22a Beta-TrCP1 WD40 domain		142	415	4.97E+01	49.7
				330	408	Cutpref						na	
				409	788	Ginzu/pdbblast	A-solenoid	1B89a Clathrin proximal leg		39	411	4.32E+01	43.2
				789	854	Ginzu/msa						2.08E+00	2.1

Table S2 • Interactions among Vps-C subunits

			Bait	CORVET									HOPS																	
				Vps3					Vps8				Vps41				Vps39													
				Vps3 1-1011 wt	Vps3 130-998	Vps3 1-492	Vps3 424-1011	Vps3 902-1001	Vps8 1-1274 wt	Vps8 422-722	Vps8 723-1187	Vps8 422-1187	Vps41 1-992 wt	Vps41 1-97	Vps41 98-500	Vps41 501-992	Vps39 1-1049 wt	Vps39 1-420	Vps39 1-618	Vps39 1-674	Vps39 1-678	Vps39 1-860	Vps39 1-903	Vps39 1-979	Vps39 421-860	Vps39 421-979	Vps39 421-1049	Vps39 861-979	Vps39 861-1049	Vps39 980-1049
	Prey	Gene	AMY	759	760	761	762	812	531	527	528	529	553	550	551	552	508	502	561	503	619	507	509	510	504	505	506	499	500	501
CORVET	Vps3	Vps3 1-1011 wt	754	0	0	0	0	0	0		0	0	0		0	0	0		0	0	0	0	0	0		0		0	0	
		Vps3 130-998	755	0	0	0	0	0	0		0	0	0		0	0	0		0	0	0	0	0	0		0		1	0	
		Vps3 1-492	756	0	0	0	0	0	0		0	0	0		0	0	0		0	0	0	0	0	0		0		0	0	
		Vps3 424-1011	757	0	0	0	0	0	0		0	0	0		0	0	0		0	0	0	0	0	0		0		0	0	
		Vps3 902-1001	811	0	0	0	0	0	0		0	0	1		0	0	0		0	0	0	0	0	0		0		0	0	
	Vps8	Vps8 1-1274 wt	571	0	0	0	0	0	0	0	0	0	0	0	0	0	0	0	0	0	0	0	0	0	0	0	0	0	0	0
		Vps8 1-421	566	0	0	0	0	0	0	0	0	0	0	0	0	0	0	0	0	0.5	0.5	0	0	0	0	0	0	0	0	0
		Vps8 422-722	567						0	0	0	0	0	0	0	0	0	0	0	0	0	0	0	0	0	0	0	0	0	0
		Vps8 422-1187	569	0	0	0	0	0	0	0	0	0	0	0	0	0	0	0	0	0	0	0	0	0	0	0	0	0	0	0
		Vps8 723-1187	568	0	0	0	0	0	0	0	0	0	0	0	0	0	0	0	0	0	0	0	0	0	0	0	0	0	0	0
		Vps8 1188-1274	570	0	0	0	0	0	0.5	0	0	0	0	0	0	0	0	0	0	0	0	0	0	0	0	0.5	0	0	0	0
HOPS	Vps41	Vps41 1-992 wt	593	0	0	0	0	0	0	0	0	0	0.5	0	0	0.5	0	0	0	0	0	0	0	0	0	0	0	0	0	0
		Vps41 1-97	590						0	0	0	0	0	0	0	0	0	0	0	0	0	0	0	0	0	0	0	0	0	0
		Vps41 98-500	591	0	0	0	0	0	0	0	0	0	0	0	0	0	0	0	0	0	1	0	1	0	0	0	0	0	0	0
		Vps41 501-992	592						0	0	0	0	0	0	0	0	0	0	0	0	0	0	0	0	0	0	0	0	0	0
	Vps39	Vps39 1-1049 wt	490	0	0	0	0	0	0	0	0	0	0	0	0	0	0	0	0	0	0	0	0	0	0	0	0	0	0	0
		Vps39 1-420	484	0	0	0	0	0	0	0	0	0.5	0	0	0	0	0	0	0	0	0.5	0	0	0	0	0	0	0	0	0
		Vps39 1-618	601	0	0	0	0	0	0	0	0	0	0	0	0	0	0	0	0	0	0	0	0.5	0	0	0	0	0	0	0
		Vps39 1-674	485	0	0	0	0	0	0	0	0	0	0	0	0	0	0	0	0	0	0	0.5	0	0	0	0	0	0	0	0
		Vps39 1-678	631	0	0	0	0	0	0.5	0	0	0	0	0	0	0	1	1	0	0	0	0	0	0.5	0	0	0	0	0	0
		Vps39 1-860	489	0	0	0	0	0	0	0	0	0	0	0	0	0	0	0	0	0	0	0	0.5	0	0	0	0	0	0	0
		Vps39 1-903	491						0	0	0	0	0	0	0	0	0	0	0	0	0	0	0	0	0	0	0	0	0	0
		Vps39 1-979	492	0	0	0	0	0	0	0	0	0	0.5	0	0	0.5	0	0	0	0	0	0	0.5	0	0	0	0	0	0	0
		Vps39 421-860	486	0	0	0	0	0	0	0	0	0	0	0	0	0.5	0	0	0	0	0	0	0	0	0	0	0	0	0	0
		Vps39 421-979	487	0	0	0	0	0	0	0	0	0	0	0	0	0	0	0	0	0	1	0	0	0	0	0	0	0	0	0
		Vps39 421-1049	488	0	0	0	0	0	0	0	0	0	0	0	0	0	0	0	0	0	0	0	0	0	0	0	0	0	0	0
		Vps39 861-979	481	0	0	0	0	0	0	0	0	0	0	0	0	0	0	0	0	0	0	0	0	0	0	0	0	0	0	0
		Vps39 861-1049	482	0	0	0	0	0	0	0	0	0	0	0	0	0	0	0	0	0	0	0	0	0	0	0	0	0	0	0
		Vps39 980-1049	483	0	0	0	0	0	0	0	0	0	0	0	0	0	0	0	0	1	1.5	0	0	0	0	0	0	0	0	0
Vps-C Core	Vps11	Vps11 1-1029 wt	574	3	3	0	3	3	0.5	0	1.5	2.5	0.5	0	0	0	3	0	0	0	0	0	0	3	0	2	0	3	3	0
		Vps11 1-350	575						0	0	0	0	0	0	0	0	0	0	0	0	0	0	0	0	0	0	0	0	0	0
		Vps11 1-475	702	0	0	0	0.5	0	0		0	0	0		0	0	0		0	0	0	0	0	0		0		0	0	
		Vps11 351-505	576	0	0	0	0.5	0	0	0	0	0	0.5	0	0	0	0	0	0	0.5	0	0	0	0	0	0	0	0	0	0
		Vps11 351-926	579	2.5	2.5	0	3	3	0	0	0	0	0	0	0	0	2	0	0	0	0	0.5	0	3	0	0.5	0	3	2	0
		Vps11 406-597	701	0	0	0	0	1	0		0	0	0		0	0	0		0	0	1	0	0	0		0		1	0	
		Vps11 506-926	577	1.5	1.5	0	3	2	0	0	0	0	0	0	0	0	0.5	0	0	0	0	0	0.5	0.5	0	0	0	2	0	0
		Vps11 736-926	705	2	1.5	0	3	2.5	0		0	0	0		0	0	3		0	0	0	0	0	3		1		2	0	
		Vps11 927-1029	578	0	0.5	0	0	0	0	0	0	0	0	0	0	0	0.5	0	0.5	0.5	0.5	0	0	0	0	0	0	0	0.5	0
	Vps18	Vps18 1-918 wt	589	0	0	0	0	0.5	0.5	0	0	0	0	0	0	0	0	0	1.5	0.5	1.5	0	0	0	0	0	0	0	0	0
		Vps18 1-337	585	0	0	0	0.5	0	0	0	0	0	0	0	0	0	0.5	0	0	0	0	0	0	0	0	0	0	0	0	0
		Vps18 1-380	586	0	0	0	0	0	0	0	0	0	0	0	0	0	0.5	0	0	0	0	0	0	0	0	0	0	0	0	0
		Vps18 338-733	587	0	0	0	1	0.5	0	0	0	0	0	0	0	0	0	0	0	0	0	0	0	0	0	0	0	0.5	0	0
		Vps18 734-918	588	0	0	0	0.5	0	0	0	0	0	0	0	0	0.5	0	0	0	0	0	0	0	0	0	0	0	0.5	0	0
	Vps16	Vps16 1-798 wt	584	0	0	0	1.5	1	0	0	0	0	0	0	0	0	0	0	0	0	0	0	0	0.5	0	0	0	0	0	0
		Vps16 1-285	580						0	0	0	0	0	0	0	0	0	0	0	0	0	0	0	0	0	0	0	0	0	0
		Vps16 1-379	581						0	0	0	0	0	0	0	0	0	0	0	0	0	0	0	0	0	0	0	0	0	0
		Vps16 286-798	582						0	0	0	0	0	0	0	0	0	0	0	0	0	0	0	0	0	0	0	0	0	0
		Vps16 479-798	583	0	0	0	0.5	1	0	0	0	0	0	0	0	0	0.5	0	0	0	0	0	0	0.5	0	0	0	0.5	0	0
SM	Vps33	Vps33 1-691 wt	596	0	0	0	0	0	0	0	0	0	0	0	0	0	0	0	0	0	0	0	0	0	0	0	0	0	0	0
		Vps33 1-177	696	0	0	0	0	0	0		0	0	0		0	0	0		0	0	0	0	0	0		0		1	0	

			Bait	Vps-C Core																				SM						
				Vps11									Vps18					Vps16					Vps33							
				Vps11 1-1029 wt	Vps11 1-350	Vps11 1-475	Vps11 351-505	Vps11 351-926	Vps11 406-597	Vps11 506-926	Vps11 583-735	Vps11 736-926	Vps18 1-918 wt	Vps18 1-337	Vps18 1-380	Vps18 338-733	Vps18 734-918	Vps16 1-798 wt	Vps16 1-285	Vps16 1-379	Vps16 286-798	Vps16 479-798	Vps33 1-691 wt	Vps33 1-25	Vps33 1-177	Vps33 26-177	Vps33 26-691	Vps33 540-629	Vps33 596-629
	Prey	Gene	AMY	534	535	683	536	539	682	537	685	686	549	545	546	547	548	544	540	541	542	543	556	763	677	678	681	679	680
CORVET	Vps3	Vps3 1-1011 wt	754	3	0	0	0	2	0	2		2	0	0		0	0	0	0	0		0	0	0	0		0		
		Vps3 130-998	755	2	0	0	0	1	0	0		1	0	0		0	0	0	0	0		0	0	0	0		0		
		Vps3 1-492	756	1	0	0	0	0	0	0		0	0	0		0	0	0	0	0		0	0	0	0		0		
		Vps3 424-1011	757	2	0	0	0	0	0	0		1	0	0		0	0	0	0	0		0	0	0	0		0		
		Vps3 902-1001	811	3	0	0	0	1	0	0		0	0	0		0	0	0	0	0		0	0	0	0		0		
	Vps8	Vps8 1-1274 wt	571	1	0	0	0	0	0	0	0	0	0	0	0	0	1	0	0	0	0	0	0	0	0	0	0	0	0
		Vps8 1-421	566	0	0	0	0	0.5	0	0	0	0	0	0	0	0	0	0	0	0	0	0	0	0	0.5	0	0	0	0
		Vps8 422-722	567	0	0	0	0	0	0	0	0	0	0	0	0	0	0	0	0	0	0	0	0		0	0	0	0	0
		Vps8 422-1187	569	2	0	0	0	0	0	0	0	0	0	0	0	0	0	0	0	0	0	0	0	0	0	0	0	0	0
		Vps8 723-1187	568	1.5	0	0	0	0	0	0	0	0	0	0	0	0	0	0	0	0	0	0	0	0	0	0	0	0	0
		Vps8 1188-1274	570	0	0	0	0	0	0	0	0	0	2.5	0	0	0	3	0	0	0	0	0	0	0	0	0	0	0	0
HOPS	Vps41	Vps41 1-992 wt	593	0	0	0	0	0	0	0	0	0	0	0	0	0	0	0	0	0	0	0	0	0	0	0	0	0	0
		Vps41 1-97	590	0	0	0	0	0	0	0	0	0	0	0	0	0	0	0	0	0	0	0	0		0	0	0	0	0
		Vps41 98-500	591	0.5	0	0	0	0.5	0	0	0	0	0	0	0	0	0	0	0	0	0	0	0	0	0	0	0	0	0
		Vps41 501-992	592	0	0	0	0	0	0	0	0	0	0	0	0	0	0	0	0	0	0	0	0		0	0	0	0	0
	Vps39	Vps39 1-1049 wt	490	2.5	0	0	0	2	0	0.5	0	1.5	0	0	0	0	0	0	0	0	0	0	0	0	0	0	0	0	0
		Vps39 1-420	484	0	0	0	0	0	0	0	0	0	0	0	0	0	0	0	0	0	0	0	0	0	0	0	0	0	0
		Vps39 1-618	601	0	0	0	0	0	0	0	0	0	0	0	0	0	0	0	0	0	0	0	0	0	0	0	0	0	0
		Vps39 1-674	485	0.5	0	0	0	0	0	0	0	0	0	0	0	0	0	0	0	0	0	0	0	0	0	0	0	0	0
		Vps39 1-678	631	0	0	0	0	0	0	0	0	0	0	0	0	0	0	0	0	0	0	0	0	0	0	0	0	0	0
		Vps39 1-860	489	0	0	0	0	0	0	0	0	0	0	0	0	0	0	0	0	0	0	0.5	0	0	0	0	0	0	0
		Vps39 1-903	491	0	0	0	0	0	0	0	0	0	0	0	0	0	0	0	0	0	0	0	0		0	0	0	0	0
		Vps39 1-979	492	2.5	0	0	0	2	0	1	0	1.5	0	0	0	0	0	0	0	0	0	0	0	0	0	0	0	0	0
		Vps39 421-860	486	0	0	0	0	0	0	0	0	0	0	0	0	0	0	0	0	0	0	0	0	0	0	0	0	0	0
		Vps39 421-979	487	0.5	0	0	0	0	0	0	0	0	0	0	0	0	0	0	0	0	0	0	0	0	0	0	0	0	0
		Vps39 421-1049	488	0.5	0	0	0	0	0	0	0	0	0	0	0	0	0	0	0	0	0	0	0	0	0	0	0	0	0
		Vps39 861-979	481	3	0	0	0	1.5	0	0	0	1	0	0	0	0	0	0	0	0	0	0	0	0	0	0	0	0	0
		Vps39 861-1049	482	3	0	0	0	2	0	0.5	0	1	0	0	0	0	0	0	0	0	0	0	0	0	0	0	0	0	0
		Vps39 980-1049	483	0	0	0	0	0	0	0	0	0	0	0	0	0	0	0	0	0	0	0	0	0	0.5	0	0	0	0
Vps-C Core	Vps11	Vps11 1-1029 wt	574	0.5	0	0	0	0.5	0	0	0	0	2	0	0	2	0	0	0	0	0	0	0	0	0	0	0	0	0
		Vps11 1-350	575	0	0	0	0	0	0	0	0	0	0	0	0	0	0	0	0	0	0	0	0		0	0	0	0	0
		Vps11 1-475	702	0	0	0	0	0	0	0		0	0	0		0	0	0	0	0		0	0	0	0		0		
		Vps11 351-505	576	0	0	0	0	0.5	0	0	0	0	0	0	0	0	0	0	0	0	0	0	0	0	0	0	0	0	0
		Vps11 351-926	579	0	0	0	0	0	0	0	0	0	0	0	0	0	0	0	0	0	0	0	0	0	0	0	0	0	0
		Vps11 406-597	701	0	0	0	0	0	0	0		0	0	0		0	0	0	0	0		0	0	0	0		0		
		Vps11 506-926	577	0	0	0	0	0	0	0	0	0	0	0	0	0	0	0	0	0	0	0	0	0	0	0	0	0	0
		Vps11 736-926	705	0	0	0	0	0	0	0		0	0	0		0	0	0	0	0		0	0	0	0		0		
		Vps11 927-1029	578	0.5	0	0.5	0	0	0	0.5	0	0	0	0.5	0	0	0.5	0.5	0.5	0.5	0	0	0.5	0	0	0	0	0	1
	Vps18	Vps18 1-918 wt	589	2.5	0	0	0	0	0	0	0	0	0	0	0	0	0	0	0	0	0	0	0	0	0	0	0	0	0
		Vps18 1-337	585	0	0	0	0	0	0	0	0	0	0	0	0	0	0	0	0	0	0	0	0	0	0	0	0	0	0
		Vps18 1-380	586	0	0	0	0	0	0	0	0	0	0	0	0	0	0	0	0	0	0	0	0	0	0.5	0	0	0	0
		Vps18 338-733	587	2.5	0	0	0	0	0	0.5	0	0	0	0	0	0	0	0	0	0	0	0	0	0	0	0	0	0	0
		Vps18 734-918	588	0	0	0	0	0	0	0	0	0	0	0	0	0	0	0	0	0	0	0	0	0	0	0	0	0	0
	Vps16	Vps16 1-798 wt	584	0	0	0	0	0.5	0	0	0	0	0	0	0	0	0	0	0	0	0	0	0	0	0	0	0	0	0
		Vps16 1-285	580	0	0	0	0	0	0	0	0	0	0	0	0	0	0	0	0	0	0	0	0		0	0	0	0	0
		Vps16 1-379	581	0	0	0	0	0	0	0	0	0	0	0	0	0	0	0	0	0	0	0	0		0	0	0	0	0
		Vps16 286-798	582	0	0	0	0	0	0	0	0	0	0	0	0	0	0	0	0	0	0	0	0		0	0	0	0	0
		Vps16 479-798	583	0.5	0	0	0	0	0	0	0	0	0	0	0	0	0	0	0	0	0	0	1.5	0	0	0	0	0	0
SM	Vps33	Vps33 1-691 wt	596	0	0	0	0	0.5	0	0	0	0	0	0	0	0	0	1.5	0	0	0	0	0	0	0	0	0	0	0
		Vps33 1-177	696	0	0	0	0	0	0	0		0	0	0		0	1	1	0	0		0	0	0	0		0		

Table S3A • Interactions of Vps-C subunits (preys) with Rab proteins (baits)

	Prey	Gene	AMY	Ypt7 wt LF	Ypt7 Q68L LF	Ypt7 T22N LF	Ypt7 D44N LF	Ypt7 D129N LF	Ypt7 N126I LF	Ypt7 I41S LF	Ypt7 T40A LF	Ypt7 wt	Ypt7 Q68L	Ypt7 T22N	Ypt7 D44N	Ypt7 D129N	Ypt7 N126I	Ypt7 I41S	Ypt7 T40A	Ypt7 K 140,147 R	Ypt7 K 5,6,48,56,140,147 R	Vps21 wt LF	Vps21 S21L LF	Vps21 Q66L LF	Vps21 wt	Vps21 S21L	Vps21 Q66L	Ypt1 wt	Sec4 wt	Ypt6 wt	Ypt10 wt	Ypt11 wt	Ypt31 wt	Ypt32 wt	Ypt52 wt	Ypt53 wt
			Bait (Rabs)	Ypt7																		Vps21						Other Rabs								
				493	494	495	496	497	498	564	565	638	647	648	649	650	651	652	653	829	830	639	640	641	533	559	560	845	846	847	784	848	849	786	850	780
CORVET	Vps3	Vps3 1-1011 wt	754									0	0	0	0	0	0	0	0	0	0				0	0	0	0	0	0	0	0	0	0	0	0
		Vps3 130-998	755									0	0	0	0	0	0	0	0	0	0				0	0	0	0	0	0	0	0	0	0	0	0
		Vps3 1-492	756									0	0	0	0	0	0	0	0	0	0				0	0	0	0	0	0	0	0	0	0	0	0
		Vps3 424-1011	757									0	0	0	0	0	0	0	0	0	0				0	0	0	0	0	0	0	0	0	0	0	0
		Vps3 901-1001	811									0	0	0	0	0	0	0	0	0	0				0	0	0	0	0	0	0	0	0	0	1	0
	Vps8	Vps8 1-1274 wt	571	0	0	0	0	0	0	0	0	0	0	0	0	0	0	0	0	0	0	1	0	2	0	0	2.5	0	0	0	0	0	0	0	0	0
		Vps8 1-421	566	0	0	0	0	0	0	0	0	0	0	0	0	0	0	0	0	0	0	0	0	0	0	0	0	0	0	0	0	0	0	0	0	0
		Vps8 422-722	567	0	0	0	0	0	0	0	0	0	0	0	0	0	0	0	0			0	0	0	0	0	0									
		Vps8 422-1187	569	0	0	0	0	0	0	0	0	0	0	0	0	0	0	0	0	0	0	0	0	1	0	0	2	0	0	0	0	0	0	0	0	0
		Vps8 723-1187	568	0	0	0	0	0	0	0	0	0	0	0	0	0	0	0	0	0	0	0	0	0	0	0	0	0	0	0	0	0	0	0	0	0
		Vps8 1188-1274	570	0	0	0	0	0	0	0	0	0	0	0	0	0	0	0	0	0	0	0	0	0	0	0	0	0	0	0	0	0	0	0	0.5	0
HOPS	Vps41	Vps41 1-992 wt	593	0	0	0	0	2	0	0	0	0	0.5	0	0	3	0.5	0	0	0	0	0	0	0	0	0	0	0	0	0	0	0	0	0	0.5	0
		Vps41 1-97	590	0	0	0	0	0	0	0	0	0	0	0	0	0	0	0	0			0	0	0	0	0	0									
		Vps41 98-500	591	0	0	0	0	0	0	0	0	0	0	0	0	0	0	0	0	0	0	0	0	0	0	0	0	0	0	0	0	0	0	0	0	0
		Vps41 501-992	592	0	0	0	0	0	0	0	0	0	0	0	0	0	0	0	0			0	0	0	0	0	0									
	Vps39	Vps39 1-1049 wt	490	0	1	0	0	2	2	2	2	0.5	0	0.5	2	3	3	3	2	2	2	0	0	0	0	0	0	0	0	0	0	0	0	0	0	0
		Vps39 1-420	484	0	0	0	0	0	0	0	0	0	0	0	0	1	0.5	1	0	0	0	0	0	0	0.5	0	0	0	0	0	0	0	0	0	0	0
		Vps39 1-618	601	0	0	0	0	0	0	2	0	0	0	0	0	1	0	1	0	0	0	0	0	0	0	0	0	0	0	0	0	0	0	0	0	0
		Vps39 1-674	485	0	0	0	0	2	1	3	2	0	0	0	1.5	3	3	3	2	1	1	0	0	0	0	0	0	0	0	0	0	0	0	0	0.5	0
		Vps39 1-678	631	0	0	0	0	2	2	3	2	0	0.5	0	2	3	3	3	2	1	1	0	0	0	0	0	0	0	0	0	0	0	0	0	0	0
		Vps39 1-860	489	2	2	2	3	3	3	3	3	2.5	2	3	3	3	3	3	3	3	3	0	0	0	0	0	0	0	0	0	0	0	0	0	0	0
		Vps39 1-903	491	0	0	0	0	0	0	0	0	0	0	0	0	0	0	0	0			0	0	0	0	0	0									
		Vps39 1-979	492	0	0	0	0	0	0	0	0	0	0	0	0	0	0	0	0	0	0	0	0	0	0	0	0	0	0	0	0	0	0	0	0.5	0
		Vps39 421-860	486	0	0	0	0	0	0	0	0	0	0	0	0	0	0	0.5	0	0	0	0	0	0	0	0	0	0	0	0	0	0	0	0	0	0
		Vps39 421-979	487	0	0	0	0	0	0	0	0	0	0	0	0	1	0.5	0.5	0	0	0	0	0	0	0	0	0	0	0	0	0	0	0	0	0	0
		Vps39 421-1049	488	0	0	0	0	0	0	0	0	0	0	0	0	0	0	0	0	0	0	0	0	0	0	0	0	0	0	0	0	0	0	0	0	0
		Vps39 861-979	481	0	0	0	0	0	0	0	0	0	0	0	0	0	0	0	0	0	0	0	0	0	0	0	0	0	0	0	0	0	0	0	0	0
		Vps39 861-1049	482	0	0	0	0	0	0	0	0	0	0	0	0	0	0	0	0	0	0	0	0	0	0	0	0	0	0	0	0	0	0	0	0	0
		Vps39 980-1049	483	0	0	0	0	0	0	0	0	0	0	0.5	0	0	0	0	0	0	0	0	0	0	0	0	0	0	0	0	0	0	0	0	0	0
Vps-C Core	Vps11	Vps11 1-1029 wt	574	0	0	0	0	0	0	0	0	0	0	0	0	0.5	0	0	0	0	0	0	0	0	0	0	0	0	0	0	0	0	0	0	0	0
		Vps11 1-350	575	0	0	0	0	0	0	0	0	0	0	0	0	0	0	0	0			0	0	0	0	0	0									
		Vps11 1-475	702									0	0	0	0	0	0	0	0	0	0				0	0	0	0	0	0	0	0	0	0	0	0
		Vps11 351-505	576	0	0	0	0	0	0	0	0	0	0	0	0	0	0	0	0	0	0	0	0	0	0	0	0	0	0	0	0	0	0	0	0	0
		Vps11 351-926	579	0	0	0	0	0	0	0	0	0	0	0	0	0	0	0	0	0	0	0	0	0	0	0	0	0	0	0	0	0	0	0	0	0
		Vps11 406-597	701									0	0	0	0	0	0	0	0	0	0				0	0	0	0	0	0	0	0	0	0	0	0
		Vps11 506-926	577	0	0	0	0	0	0	0	0	0	0	0	0	0	0	0	0	0	0	0	0	0	0.5	0	0	0	0	0	0	0	0	0	0.5	0
		Vps11 736-926	705									0	0	0	0	0	0	0	0	0	0				1	0	0	0	0	0	0	0	0	0	0.5	0
		Vps11 927-1029	578	0	0	0	0	0	0	0	0	0	0	0	0	0	0	0	0	0	0	0	0	0	1	0.5	0	0	0	0	0	1	0	0	0	0
	Vps18	Vps18 1-918 wt	589	0	0	0	0	0	0	0	0	0	0	0	0	0	0	0	0	0	0	0	0	0	0	0	0	0	0	0	0	0	0	0	0	0
		Vps18 1-337	585	0	0	0	0	0	0	0	0	0	0	0	0	0	0	0	0	0	0	0	0	0	0	0	0	0	0	0	0	0	0	0	0	0
		Vps18 1-380	586	0	0	0	0	0	0	0	0	0	0	0	0	0	0	0	0	0	0	0	0	0	0	0	0	0	0	0	0	0	0	0	0	0
		Vps18 338-733	587	0	0	0	0	0	0	0	0	0	0	0	0	0	0	0	0	0	0	0	0	0	0	0	0	0	0	0	0	0	0	0	0	0
		Vps18 734-918	588	0	0	0	0	0	0	0	0	0	0	0	0	0	0	0	0	0	0	0	0	0	0	0	0	0	0	0	0	0	0	0	0.5	0
	Vps16	Vps16 1-798 wt	584	0	0	0	0	0	0	0	0	0	0	0	0	0	0	0	0	0	0	0	0	0	0	0	0	0	0	0	0	0	0	0	0	0
		Vps16 1-285	580	0	0	0	0	0	0	0	0	0	0	0	0	0	0	0	0			0	0	0	0	0	0									
		Vps16 1-379	581	0	0	0	0	0	0	0	0	0	0	0	0	0	0	0	0			0	0	0	0	0	0									
		Vps16 286-798	582	0	0	0	0	0	0	0	0	0	0	0	0	0	0	0	0			0	0	0	0	0	0									
		Vps16 479-798	583	0	0	0	0	0	0	0	0	0	0	0	0	0	0	0	0	0	0	0	0	0	0	0	0	0	0	0	0	0	0	0	0.5	0
SM	Vps33	Vps33 1-691 wt	596	0	0	0	0	0	0	0	0	0	0	0	0	0	0	0	0	0	0	0	0	0	0	0	0	0	0	0	0	0	0	0	0.5	0
		Vps33 1-177	696									0	0	0	0	0	0	0	0	0	0				0	0	0	0.5	0	0	0	0	0	0	0	0.5

Table S3B • Interactions of Vps-C subunits (baits) with Rab proteins (preys)

Bait: CORVET (Vps3, Vps8); HOPS (Vps41, Vps39); Vps-C Core (Vps11, Vps18, Vps16); SM (Vps33). Prey: Rabs (Ypt7, Vps21, Other).

Prey (Rabs)	Gene	AMY	Vps3 1-1011 wt (759)	Vps3 130-998 (760)	Vps3 1-492 (761)	Vps3 424-1011 (762)	Vps3 901-1001 (812)	Vps8 1-1274 wt (531)	Vps8 422-722 (527)	Vps8 723-1187 (528)	Vps8 422-1187 (529)	Vps41 1-992 wt (553)	Vps41 1-97 (550)	Vps41 98-500 (551)	Vps41 501-992 (552)
Ypt7	Ypt7 wt LF	475						0	0	0	0	0	0	1	0
Ypt7	Ypt7 Q68L LF	476						0	0	0	0	0	0	0	0
Ypt7	Ypt7 T22N LF	477						0	0	0	0	0	0	0	0
Ypt7	Ypt7 D44N LF	478						0	0	0	0	0	0	0	0
Ypt7	Ypt7 D129N LF	479						0	0	0	0	0	0	0	0
Ypt7	Ypt7 N126I LF	480						0	0	0	0	0	0	0	0
Ypt7	Ypt7 I41S LF	604						0	0	0	0	0	0	0	0
Ypt7	Ypt7 T40A LF	605						0	0	0	0	0	0	0	0
Ypt7	Ypt7 wt	634	0	0	0	0	0	0	0	0	0	1	0	3	0
Ypt7	Ypt7 Q68L	654	0	0	0	0	0	0		0	0	0	0	0	0
Ypt7	Ypt7 T22N	655	0	0	0	0	0	0		0	0	0	0	0	0
Ypt7	Ypt7 D44N	656	0	0	0	0	0	0		0	0	0	0	0	0.5
Ypt7	Ypt7 D129N	657	0	0	0	0	0	0		0	0	0	0	0	0.5
Ypt7	Ypt7 N126I	658	0	0	0	0	0	0		0	0	0	0	0.5	0
Ypt7	Ypt7 I41S	659	0	0	0	0	0	0		0	0	0	0	0	0
Vps21	Vps21 wt LF	635						1	0	0	1	0	0	0	0
Vps21	Vps21 S21L LF	636						0	0	0	0	1	0	0	0
Vps21	Vps21 Q66L LF	637						0	0	0	1	0	0	0	0
Vps21	Vps21 wt	573	0	0	2	0	0	1.5	0	0	2	0	0	0	0
Vps21	Vps21 S21L	599	0	0	0	0	0	0	0	0	0	1	0	0	0
Vps21	Vps21 Q66L	600	0	0	1.5	0	0	2.5	0	0	2.5	0	0	0	0
Other	Ypt1 wt	884	0	0	0	0	0	0		0	0	0		0	0
Other	Sec4 wt	861	0	0	0	0	0	0		0	0	0		0	0
Other	Ypt6 wt	862	0	0	0	0	0	0		0	0	0		0	0
Other	Ypt10 wt	863	0	0	0	0	0	0		0	0	0		0	0
Other	Ypt11 wt	864	0	0	0	0	0	0		0	0	0		0	0
Other	Ypt31 wt	865	0	0	0	0	0	0		0	0	0		0	0
Other	Ypt32 wt	866	0	0	0	0	0	0		0	0	0		0	0
Other	Ypt52 wt	778	0	0	0	0	0	0		0	0	0		0	0
Other	Ypt53 wt	868	0	0	0	0	0	0		0	0	0		0	0

Prey (Rabs)	Gene	AMY	Vps39 1-1049 wt (508)	Vps39 1-420 (502)	Vps39 1-618 (561)	Vps39 1-674 (503)	Vps39 1-678 (619)	Vps39 1-860 (507)	Vps39 1-903 (509)	Vps39 1-979 (510)	Vps39 421-860 (504)	Vps39 421-979 (505)	Vps39 421-1049 (506)	Vps39 861-979 (499)	Vps39 861-1049 (500)	Vps39 980-1049 (501)
Ypt7	Ypt7 wt LF	475	0	0	0	2	1	0	2	0	0	0	0	0	0	0
Ypt7	Ypt7 Q68L LF	476	0	0	0	3	1	2	2	0	0	0	0	0	0	0
Ypt7	Ypt7 T22N LF	477	0	0	0	0	0	0	1	0	0	0	0	0	0	0
Ypt7	Ypt7 D44N LF	478	1	0	0	3	2	2	3	0	0	0	0	0	0	0
Ypt7	Ypt7 D129N LF	479	1	0	0	3	3	3	3	0	0	0	0	0	0	0
Ypt7	Ypt7 N126I LF	480	0	0	0	2	2	0	2	0	0	0	0	0	0	0
Ypt7	Ypt7 I41S LF	604	2	0	0	3	3	3	3	0	0	0	0	0	0	0
Ypt7	Ypt7 T40A LF	605	0	0	0	0	0	0	0	0	0	0	0	0	0	0
Ypt7	Ypt7 wt	634	0.5	0	1.5	2	2.5	2	1.5	0	0	0	0	0	0	0
Ypt7	Ypt7 Q68L	654	2		0	2.5	2.5	2	3	0		0		0	0	
Ypt7	Ypt7 T22N	655	0		0	0.5	0	0	1	0		0		0	0	
Ypt7	Ypt7 D44N	656	0		0.5	1	2	0	2	0		0		0	0	
Ypt7	Ypt7 D129N	657	2		0	3	3	3	3	1		0		0	0	
Ypt7	Ypt7 N126I	658	1		0	0.5	1	2	2	0		0		0	0	
Ypt7	Ypt7 I41S	659	2		0	3	3	3	3	0		0		0	0	
Vps21	Vps21 wt LF	635	0	0	0	0	0	0	0	0	0	0	0	0	0	0
Vps21	Vps21 S21L LF	636	0	0	0	0	0	0	0	0	0	0	0	0	0	0
Vps21	Vps21 Q66L LF	637	0	0	0	0	0	0	0	0	0	0	0	0	0	0
Vps21	Vps21 wt	573	0	0	0	0.5	0	0	0	0	0	0	0	0	0	0
Vps21	Vps21 S21L	599	0	0	0	0	0	0	0.5	0	0	0	0	0	0	0
Vps21	Vps21 Q66L	600	0	0	0	0	0	0	0	0	0	0	0	0	0	0
Other	Ypt1 wt	884	0		0	0	0	0	0	0		0		0	0	
Other	Sec4 wt	861	0		0	0	0	0	0	0		0		0	0	
Other	Ypt6 wt	862	0		0	0	1	1	1	0		0		0	0	
Other	Ypt10 wt	863	0		0	0	0	0	0	0		0		0	0	
Other	Ypt11 wt	864	0		0	0	1	0	0	0		0		0	0	
Other	Ypt31 wt	865	0		0	0	0	0	0	0		0		0	0	
Other	Ypt32 wt	866	1		0	1	2	2	2	0		0		0	0	
Other	Ypt52 wt	778	0		0	0	0	0	0	0		0		0	0	
Other	Ypt53 wt	868	0		0	0	0	0	0	0		0		0	0	

Prey (Rabs)	Gene	AMY	Vps11 1-1029 wt (534)	Vps11 1-350 (535)	Vps11 1-475 (683)	Vps11 351-505 (536)	Vps11 351-926 (539)	Vps11 406-597 (682)	Vps11 506-926 (537)	Vps11 583-735 (685)	Vps11 736-926 (686)	Vps18 1-918 wt (549)	Vps18 1-337 (545)	Vps18 1-380 (546)	Vps18 338-733 (547)	Vps18 734-918 (548)	Vps16 1-798 wt (544)	Vps16 1-285 (540)	Vps16 1-379 (541)	Vps16 286-798 (542)	Vps16 479-798 (543)	Vps33 1-691 wt (556)	Vps33 1-25 (763)	Vps33 1-177 (677)	Vps33 26-177 (678)	Vps33 26-691 (681)	Vps33 540-629 (679)	Vps33 596-629 (680)
Ypt7	Ypt7 wt LF	475	0	0	0	0	0	0	0	0	0	0	0	0	0	0	0	0	0	0	0	0		0	0	0	0	0
Ypt7	Ypt7 Q68L LF	476	0	0	0	0	0	0	0	0	0	0	0	0	0	0	0	0	0	0	0	0		0	0	0	0	0
Ypt7	Ypt7 T22N LF	477	0	0	0	0	0	0	0	0	0	0	0	0	0	0	0	0	0	0	0	0		0	0	0	0	0
Ypt7	Ypt7 D44N LF	478	0	0	0	0	0	0	0	0	0	0	0	0	0	0	0	0	0	0	0	0		0	0	0	0	0
Ypt7	Ypt7 D129N LF	479	0	0	0	0	0	0	0	0	0	0	0	0	0	0	0	0	0	0	0	0		0	0	0	0	0
Ypt7	Ypt7 N126I LF	480	0	0	0	0	0	0	0	0	0	0	0	0	0	0	0	0	0	0	0	0		0	0	1	0	0
Ypt7	Ypt7 I41S LF	604	0	0	0	0	0	0	0	0	0	0	0	0	0	0	0	0	0	0	0	0		0	0	0	0	0
Ypt7	Ypt7 T40A LF	605	0	0	0	0	0	0	0	0	0	0	0	0	0	0	0	0	0	0	0	0		0	0	0	0	0
Ypt7	Ypt7 wt	634	0	0	0	1	0	0	0	0	0	0	0	0	0	0	0	0	0	0	0	1.5	0	1.5	0	0	0	0
Ypt7	Ypt7 Q68L	654	0	0	0	0	0	0	0	0	0	0	0	0	0	0	0	0	0	0	0	0	0	0	0	0	0	0
Ypt7	Ypt7 T22N	655	0	0	0	0	0	0	0	0	0	0	0	0	0	0	0	0	0	0	0	0.5	0	0	0	0	0	0
Ypt7	Ypt7 D44N	656	0	0	0	1	0	0	0	0	0	0	0	0	0	0	0	0	0	0	0	1	0	1.5	0	0.5	0	0
Ypt7	Ypt7 D129N	657	0	0	0	0	0	0	0	0	0	0	0	0	0	0	0	0	0	0	0	0	0	0	0	0	0	0
Ypt7	Ypt7 N126I	658	0	0	0	0	0	0	0	0	0	0	0	0	0	0	0	0	0	0	0	0	0	0.5	0	0	0	0
Ypt7	Ypt7 I41S	659	0	0	0	0	0	0	0	0	0	0	0	0	0	0	0	0	0	0	0	0	0	0	0	0	0	0
Vps21	Vps21 wt LF	635	0	0	0	0	0	0	0	0	0	0	0	0	0	0	0	0	0	0	0	0		0	0	0	0	0
Vps21	Vps21 S21L LF	636	0	0	0	0	0	0	0	0	0	0	0	0	0	0	0	0	0	0	0	0		0	0	0	0	0
Vps21	Vps21 Q66L LF	637	0	0	0	0	0	0	0	0	0	0	0	0	0	0	0	0	0	0	0	0		0	0	0	0	0
Vps21	Vps21 wt	573	0	2.5	2	0	0	0	0	0	0	0	0	0	0	0	0	0	0	0	0	0	0	0	0	0	0	0
Vps21	Vps21 S21L	599	0	0	0	0	0	0	0	0	0	0	0	0	0	0	0	0	0	0	0	0	0	0	0	0	0	0
Vps21	Vps21 Q66L	600	0	0	0	0	0	0	0	0	0	0	0	0	0	0	0	0	0	0	0	0	0	0	0	0	0	0
Other	Ypt1 wt	884	0	0	0	0	0	0	0		0	0	0		0	0	0	0	0		0	0	0	0		0		
Other	Sec4 wt	861	0	0	0	0	0	0	0		0	0	0		0	0	0	2	1		1	0	0	0		0		
Other	Ypt6 wt	862	0	0	0	0	0	0	0		0	0	0		0	0	0	0	0		0	1	0	2		0		
Other	Ypt10 wt	863	0	0	0	0	0	0	0		0	0	0		0	0	0	0	0		0	0	0	0		0		
Other	Ypt11 wt	864	0	0	0	0	0	0	0		0	0	0		0	0	0	0	0		0	0	0	0		0		
Other	Ypt31 wt	865	0	0	0	0	0	0	0		0	0	0		0	0	0	0	0		0	0	0	0		0		
Other	Ypt32 wt	866	0	0	0	0	0	0	0		0	0	0		0	0	0	0	0		0	0	0	0		0		
Other	Ypt52 wt	778	0	0	0	0	0	0	0		0	0	0		0	0	0	0	0		0	0	0	0		0		
Other	Ypt53 wt	868	0	0	0	0	0	0	0		0	0	0		0	0	0	0	0		0	0	0	0		0		

Table S4. Phenotypes resulting from HOPS/CORVET truncations

A. CPY and ALP maturation

Genotype	CPY	ALP
Wild-type	Mature	Mature
pep4Δ prb1Δ	Pro [p2]	Pro-
vps11$^{736\Delta}$	Pro [p2]	Pro-
vps11$^{926\Delta}$ (ΔRING)	Mature	Pro-
vps18$^{826\Delta}$ (ΔRING)	Pro [p2]	Pro-
vps8$^{1188\Delta}$ (ΔRING)	Mature & Pro [p2]	Mature
vps3$^{900\Delta}$	Pro [p2]	Mature & Pro-
vps39$^{860\Delta}$	Mature & Pro [p2]	Pro-
vps39$^{979\Delta}$ (ΔRING)	Mature & Pro [p2]	Mature & Pro-

B. CPY missorting

Genotype	CPY-invertase secretion
Wild-type	None
pep4Δ prb1Δ	None
vps3Δ	Strong
vps3$^{900\Delta}$	Strong
vps11Δ	Strong
vps11$^{1\text{-}735\Delta}$	Strong
vps11$^{926\Delta}$ (ΔRING)	Weak

***C. Complementation of vps11*$^{735\Delta}$ *sorting defects by vps11*$^{736\text{-}1029}$**

Genotype	CPY	ALP	GFP-CPS
Wild-type	Mature	Mature	Vacuole lumen
vps11Δ	Pro [p2]	Pro-form	N/A
vps11$^{735\Delta}$	Pro [p2]	Pro-form	N/A
vps11$^{736\text{-}1029}$	Pro [p2]	Pro-form	N/A
vps11$^{735\Delta}$ + *vps11*$^{736\text{-}1029}$	Mature	Mature	Vacuole lumen

Table S5 Strains used in this study

Strain	Genotype	Source
PJ694a	*MATa trp1-901, leu2-3,112, ura3-52, his3-200 gal4Δ, gal80Δ, LYS2::GAL1-HIS3, GAL2-ADE2, met2::GAL7, -lacZ*	James *et al.,* 1996
PJ694α	*MATα trp1-901, leu2-3,112, ura3-52, his3-200 gal4Δ, gal80Δ, LYS2::GAL1-HIS3, GAL2-ADE2, met2::GAL7, -lacZ*	James *et al.,* 1996
BY4742	*MATα his3Δ1 leu2Δ0 lys2Δ0 ura3Δ0*	ATCC
AMY942	BY4742; *vps39Δ::KanMX4*	This study
AMY885	BY4742; *vps39-860Δ::URA3*	This study
AMY886	BY4742; *vps39-979Δ::URA3*	This study
AMY1106	BY4742; *vps11Δ::KanMX4*	This study
AMY1107	BY4742; *vps11-350Δ::KanMX4*	This study
AMY1108	BY4742; *vps11-445Δ::KanMX4*	This study
AMY1109	BY4742; *vps11-505Δ::KanMX4*	This study
AMY1199	BY4742; *vps11-735Δ::KanMX4*	This study
AMY1198	BY4742; *vps11-926Δ::KanMX4*	This study
BJ8987	*MATα vps8-200 ura3-52 trp1 leu2Δ1 his3Δ200*	Jones *et al.,* 1998
BJ4490	*MATa pep5 (vps11Δ445)::TRP1 vps8-200 leu2Δ1 trp1Δ101*	Jones *et al.,* 1998
BJ6919	*MATa pep5 (vpsΔ445)::TRP1 leu2Δ1 trp1 ade6*	Jones *et al.,* 1998
BJ8866	*MATa leu2Δ1 ura3-52 trp1*	Jones *et al.,* 1998
AMY1113	*MATα vps8-200 ura3-52 trp1 leu2Δ1 his3Δ200 vps11-445Δ::KanMX4*	This study
SEY6210	*MATα leu2-3,112 ura3-52 his3-Δ200 trp1-Δ901 lys2-801 suc2-Δ9*	Robinson *et al.,* 1988
BHY10	*MATα leu2-3,112 ura3-52 his3-Δ200 trp1-Δ901 lys2-801 suc2-Δ9 CPY-invertase::LEU2*	Horazdovsky *et al.,* 1994
DNY356	*MATα leu2-3,112 ura3-52 his3-Δ200 trp1-Δ901 lys2-801 suc2-Δ9 CPY-invertase::LEU2 vps11Δ::KanMX4*	This study
DNY357	*MATα leu2-3,112 ura3-52 his3-Δ200 trp1-Δ901 lys2-801 suc2-Δ9 CPY-invertase::LEU2 vps11-926Δ::KanMX4*	This study
DNY358	*MATα leu2-3,112 ura3-52 his3-Δ200 trp1-Δ901 lys2-801 suc2-Δ9 CPY-invertase::LEU2 vps11-735Δ::KanMX4*	This study